
Review

Ultrasonic Guided-Waves Sensors and integrated Structural Health Monitoring systems for impact detection and localization: a review

Lorenzo Capineri * and Andrea Bulletti

Department of Information Engineering, University of Florence, Via S. Marta 3, 50139, Firenze, Italy; andrea.bulletti@unifi.it, lorenzo.capineri@unifi.it

Correspondence: lorenzo.capineri@unifi.it

Abstract: This review article is focused on the analysis of the state of the art of sensors for guided ultrasonic waves for the detection and localization of impacts, therefore of interest for the structural health monitoring (SHM). The recent developments in sensor technologies are then reported and discussed through the many references in recent scientific literature. The physical phenomena related to impact event and the main physical quantities are then introduced to discuss their importance in the development of the hardware and software components for SHM systems. An important aspect of the article is the description of the different ultrasonic sensor technologies currently present in the literature and what advantages and disadvantages they could bring, in relation to the various phenomena investigated. In this context, the analysis of the front-end electronics is deepened, the type of data transmission both in terms of wired and wireless technology and in terms of online and offline signal processing. The integration aspects of sensors for the creation of networks with autonomous nodes with the possibility of powering through energy harvesting devices and the embedded processing capacity is also studied. Finally, the emerging sector of processing techniques using deep learning and artificial intelligence concludes the review by indicating the potential for the detection and autonomous characterization of the impacts.

Keywords: structural health monitoring (SHM); acoustic emission, guided waves; Lamb waves; sensors; ultrasound; piezoelectric; composites; piezopolymers; PVDF; interdigital transducer (IDT); PWAS; CMUT; mems; analog electronic front end; analog signal processing; impact localization; impact detection; sensor node; wireless sensor networks (WSN); IoT; deep learning; artificial intelligence.

1 Introduction

Structural health monitoring (SHM) is a rapidly evolving field and there is a vast literature covering several topics related to this field, including several excellent reviews. The motivations of this paper are to report the recent developments on technologies, especially sensors and mixed signal electronic interfaces, that enable the integration into a sensor node. The sensor node concept is analyzed in this review and perspective integration with the monitored structures is examined. In the

introduction are reported the main concepts behind the design of a SHM system for impact monitoring and the reader can find related reviews. Later in the introduction, the main system components are defined and in the following sections they will be discussed more deeply.

Ultrasonic non-destructive investigation (NDI) methods based on the principle of acoustic emission (AE) have evolved over the past two decades towards structural monitoring systems with guided ultrasonic waves [1,2], driven by applications in the aerospace, civil engineering, energy conversion and transportation systems automotive (e.g. wind turbines, pipelines, liquid natural gas cylinders). The safety of the structure and the prediction of life or maintenance are the key elements that must be provided by SHM systems and the main concept behind were explained in a comprehensive work by Farrar and Worden [3] and in a related book [4]. Among several type of defects, for example breakages due to fatigue, mechanical and thermal stresses, impacts with objects, etc. are all possible causes of damaging. The damage are sometimes not visible because it is internal to the structure or small but not without importance from the point of view of the safety and reliability of the operation of the system. To avoid catastrophic accidents the damage prognosis is an essential task connected to the impact events; a framework for the damage prognosis was described in chapter 14 of the book published by Farrar and Worden [5].

Non-Destructive Testing (NDT) is a wide group of analysis techniques used in science and technology industry to evaluate the properties of a material, component, or system without causing damage and is often carried out in laboratory or on site on a scheduled program. SHM, unlike NDT, requires the installation of sensors/transducers operating in the environment in which the structure

operates under remote control and for this reason the realization of such systems requires a considerable effort of integration of several disciplines:

- (1) modelling of damage physical phenomena and their influence on the physical sensed quantities,
- (2) sensors including calibration and self-diagnostics,
- (3) front-end electronics including embedded processing,
- (4) data transmission (wired, wireless),
- (5) online (or real time) or offline signal/image processing,
- (6) impact event detection and localization
- (7) damage detection and classification techniques based on database processing,
- (8) prognostics,
- (9) artificial intelligence (AI)/machine learning (ML) for automatic damage detection and progression evaluation.

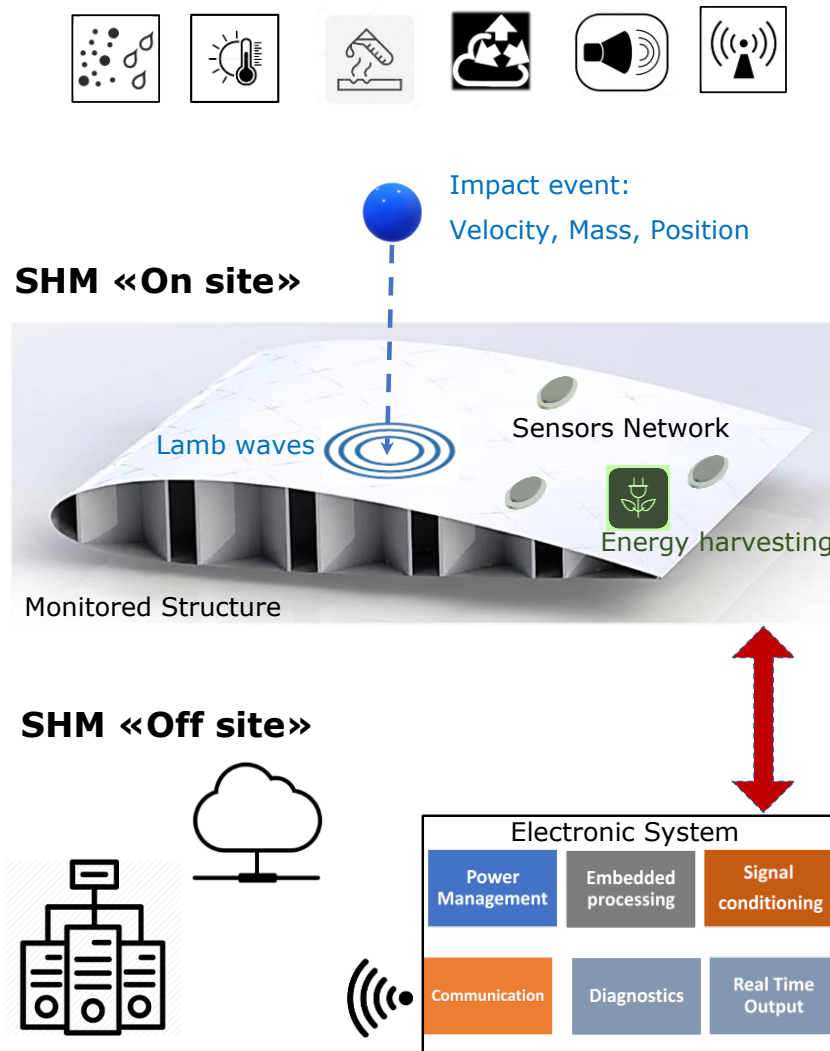


Figure 1 Graphical representation of an advanced SHM system for impact monitoring. (Top) Environmental conditions (dust, moisture, temperature, pressure, vibrations, electromagnetic interference) and impact events characterized by the object mass, velocity, shape and dimensions. (Centre) On-site components of the SHM system subjected to environment conditions installed on the monitored structure (e.g., a section of a composite airplane wing). (Bottom) Off-site components installed remotely and connected to the sensors network; the Electronic System can operate in a protected environment (e.g., inside airplane fuselage) with real-time processing capability. Off-line signal/data processing based on big data archive with workstations connected to the web for software applications of AI/ML and prognostics.

Following the above list of specific topics, in Figure 1 are illustrated the different components of an SHM system and their interaction: the environmental conditions, the on-site hardware and the off-site hardware and software resources. The different characteristics of the structures (dimensions, materials, environmental conditions) and their structural monitoring systems (cost, footprint, weight, power consumption, safety and reliability criteria, response/update times) often require the

design of ad hoc systems by exploiting multidisciplinary knowledge in electronics, informatics, telecommunications, and finally material technology and mechanical properties.

For a general understanding of the state of the art, the reader can refer to the review paper of Mitra et al. [6], where several publications relating to the various components of an SHM system are discussed (see above list of nine points). In that paper are considered the various monitoring techniques based on ultrasonic guided waves (UGW) piezoelectric and fibre optic sensors, laser vibrometry (SLDV) techniques and others. In addition, indications are given of what research and development lines may be for advanced SHM systems. As already introduced in this paragraph, monitoring techniques based on UGW by piezoelectric transducers are among the most common and most developed since they have a longer history [7] than SHM systems based on optical sensors, in particular Fiber Bragg Grating (FBG) sensors; for completeness the evolution of state of the art for optoelectronic sensors is reported in [8–12] but is not discussed further in this paper. Similarly, the evolution of piezoelectric materials for the realization of sensors and actuators of UGW, the development of integrated electronic components and systems with low power consumption, makes it necessary a continuous updating of the research to provide possible design methodologies, technologies, to bring SHM systems increasingly widespread and tested in the field. Although many published papers report the outcomes obtained with laboratory set-up of guided ultrasonic wave SHM systems, their demonstration in the field is still limited. For the latter problem, there are various reasons but certainly one of these is the complexity of the installation of the sensors on a target structure, the real time signal acquisition and processing and the replication of the real-life environmental conditions. An interesting reference for the testing of SHM systems in the aerospace industry is

provided in a report presented by Dennis Roach of Sandia National Labs [13]: this report shows the objectives and implementations of SHM systems for airplanes and includes several examples with piezoelectric and fibre optic sensor applications for monitoring impacts, deformations, debonding, delamination and damage progression.

Finally, it is useful to point out the effort made to create standards for the development of systems and methods for SHM and NDT based on acoustic emission, especially for the rapidly evolving SHM sector and for example the British Standard for Acoustic Emission and Condition Monitoring can be found in The Official Yearbook of the British Institute of Non-Destructive Testing [14].

After this introduction of the background of SHM systems based on UGW in active and passive modes, the present paper focuses the elements of the system shown in Figure 1 for the implementation of impact monitoring advanced systems on metal and composite materials with UGW piezoelectric sensors. In this paper we consider primarily piezoelectric sensors used for impact detection in passive (“listening”) mode but also in combination with the transducers operating in active mode for the investigation of damage and its progression over time. The trend of integrating different sensors types (UGW, FBG, accelerometer, strain, temperature, etc.) into a node increases the information about the impact and the operational conditions of the sensors that are influenced by the environment leading to the concept of a “multifunctional sensor node”.

The evolution from the common AE monitoring configuration with a layout of sparse single element sensors with off-the shelf electronics to the recent design of sensors networks with “smart-sensor nodes”, requires a continuous analysis and evaluation of the progresses in several fields.

This work first presents a review of methodological developments about the criteria to be adopted for the elaboration of impact-generated Lamb wave modes (Section 2). Then, it addresses technological developments about UGW sensors and actuators including new materials and sensor types with a focus on microfabrication technologies (Section 3), front-end analog-digital electronics and power management (Section 4) and the integration wired or wireless sensor networks (WSN) with real-time acquisition and signal processing capabilities for monitoring environmental parameters (Section 5). Finally, the authors believe relevant to report in Section 6 the recent applications of Artificial Intelligence (AI) and Machine Learning (ML) for autonomous detection and positioning of impact events. In the Conclusions, we will draw guidance on research topics and challenges in the various areas covered by sections 2 to 6. To ease the reader interested in selected topics tackled in this paper, an acronym list is reported in Appendix A; the list also shows acronyms that are recently introduced in the literature by new technologies and methodologies adopted in this multidisciplinary field and the reader can familiarized with.

2. Characteristics of signals generated by impacts on planar structures relevant to the design of SHM systems.

2.1 Dispersion and attenuation of Lamb waves.

In this section are discussed the implication of the attenuation and dispersion characteristics of UGW relevant for the design and implementation of a SHM system. The interested reader can find main references for the theory and modelling of ultrasonic guided waves [1] and [15]. In brief we remember that ultrasonic waves guided for SHM, are mechanical waves that propagate within a material delimited by an interface with a different medium. Propagation within the space-limited structure simultaneously produces dispersive modes of propagation in frequency. In the case of

structures with thicknesses comparable to wavelength, such as thin planar structures, propagation modes have symmetrical and antisymmetric characteristics with respect to the axis of symmetry of the structure and are determined by the theory behind Lamb waves, as explained in [16]. For an isotropic and homogeneous laminate material as aluminium, we illustrate the dispersion characteristics in **Figure 2** (top) by the calculated phase velocities for the different guided modes versus the *frequency x thickness* product (fxd). Another difference between these two UGW modes is the dependence on frequency attenuation as show in **Figure 2** (bottom): the S_0 mode is remarkably attenuated in the low frequency range and for the reception of this mode is necessary a high pass filtering and amplifier gain to be separated from the slower and higher amplitude components of the A_0 mode.

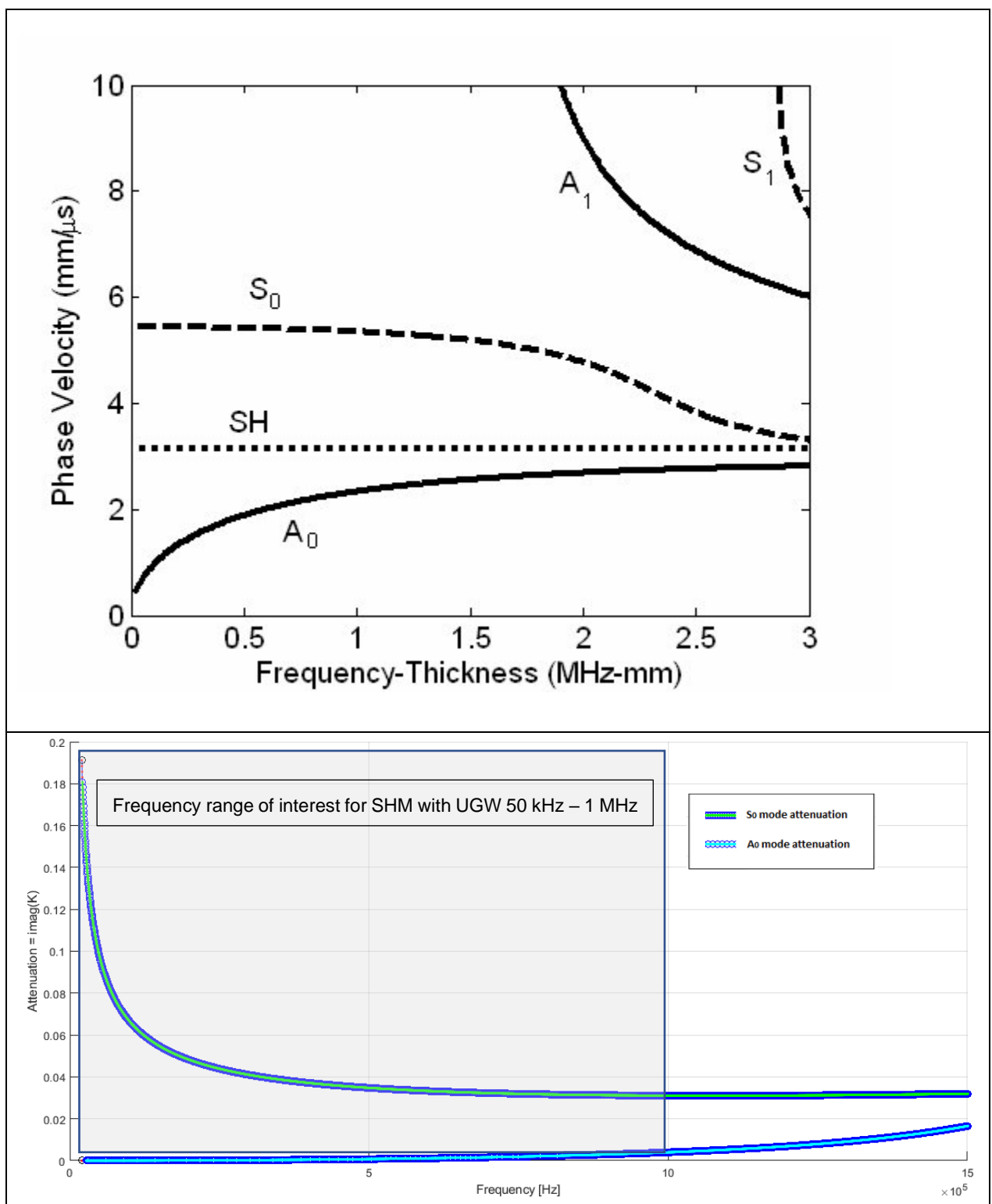


Figure 2 – (Top) Dispersion curves of phase velocity for low order modes Symmetric (S_0), Antisymmetric (A_0) and Shear Horizontal (SH) in an aluminium plate. The diagram shows that higher order modes (A_1 , S_1 , etc.) are generated above the cut-off value of

1.5MHz x mm. (Bottom) Frequency dependent attenuation of Symmetric (S_0) and Antisymmetric (A_0) modes calculated as imaginary part of the complex wavenumber K for an aluminium plate 1.4 mm thick [1].

The propagation of symmetrical modes within a planar structure is therefore a two-dimensional phenomenon; the propagation of the various modes is subjected to attenuation that mainly follows the law of geometric decay inversely at the root of the distance. Author in [15] proposed a deep and comprehensive analysis of the attenuation phenomena that are basic to differentiate the design of SHM systems according to the characteristics of the different materials (composite or metallic) and the size of the structure; thus attenuation analysis is essential to define the distance and area coverage with a certain type of transducer/sensor without exceeding the attenuation limit (50-70 dB), that results difficult to deal with analog-front-end (AFE) electronic based on COTS, unless acceptable expensive and complex electronic customized design. Indicatively, the operating frequencies for Lamb's guided ultrasonic waves range from 100 kHz to 1 MHz, and in this wide range a compromise must be found between attenuation, wavelength, minimum detectable impact energy, and for the transducers/sensors the size, type, sensitivity and bandwidth. To solve these problems, methods for optimizing the position of transducers have recently been proposed by Mallardo et al. [17] based on the background of UGW propagation theory; in this work a method is developed to define the optimal positions considering the characteristics of the material and sensors thus also optimizing the number of sensors transducers, while concluding that there is no general solution to the problem since each application has different constraints and therefore requires a series of a priori choices.

2.2. - Ultrasonic guided waves generated by different velocity of impacts on isotropic elastic plates.

Impact monitoring systems can be designed for different applications where impacts with different objects hitting the structure have different energy, mass, velocity. It is of interest to explain the

different effects on UGWs generated by impacts at different velocity. There are several categories of impact loading: low velocity (large mass), intermediate velocity, high/ballistic velocity (small mass), and hyper velocity impacts. These categories of impact loading are important because there are remarkable differences in energy transfer between the object and target, energy dissipation and damage propagation mechanisms as the velocity of the object varies. According to the literature, low velocity impacts occur typically at a velocity below 10 m/s, intermediate impacts occur between 10 m/s and 50 m/s, high velocity (ballistic) impacts have a range of velocity from 50 m/s to 1000 m/s, and hyper velocity impacts have the range of 2 km/s to 5 km/s [18].

In several studies [19–21] signals generated by non-destructive impacts have been treated, that is, they do not cause any damage to the laminate under examination neither with single impact nor with multiple impacts, however no information is given on the extent of impact. Furthermore, in [22] the impacts are distinguished based on the potential energy of the impacting bodies with values ranging from 500 mJ to 3.5 mJ. In other early studies on this subject [23,24] the impacts are instead distinguished based on the impact velocity.

The study of impacts that occur in an isotropic elastic flat plate is based on following assumptions:

- The ultrasonic signal generated by an impact is a guided wave signal that propagates into the plate without energy loss [19,25].
- The frequency content of the ultrasonic signals generated by impacts depends on the impact velocity [26] [23] and is not modified during the propagation inside the plate [27].

According to the above assumptions we can remark that the main feature of the signals generated by impacts is the impact velocity that also determines the amplitude of the Lamb waves. From the physics laws for a falling body from a certain height, the potential energy is converted in kinetic energy; the impact velocity v_i can be calculated by knowing the kinetic energy E_k and the mass m of the impacting object as reported in the following formula:

$$v_i = \sqrt{\frac{2E_k}{m}} \quad (1)$$

The study reported in [23] shows that two fundamental propagation modes can be distinguished in impact phenomena: a slow propagation mode (flexural mode or A_0 mode) and a fast propagation mode (extensional mode or S_0 mode). The amplitude of the A_0 mode signal is dominant respect to the S_0 mode but the amplitude of the S_0 mode signal can be much significative based on the impact velocity: the higher the impact speed is and, on the consequent, higher is the amplitude of the signal relative to the S_0 mode.

Authors in [23] also reported an acquired signal from a high-speed impact (700m/s) where they demonstrate that applying a low-pass filter with (with a cut-off frequency of 800kHz), it is possible to extract only the two fundamental propagation modes (A_0 and S_0) and in this case the amplitude of the S_0 mode becomes comparable to that of the A_0 mode. According to the author experience, we investigated the possibility to extrapolate the S_0 mode signal also in low velocity impacts by applying a low-pass filter in the analogic front-end electronic board with proper cut-off frequency. Figure 3 shows ultrasonic signals generated by a low-velocity impact (about 3m/s) on an aluminium plate with thickness 1.5 mm.

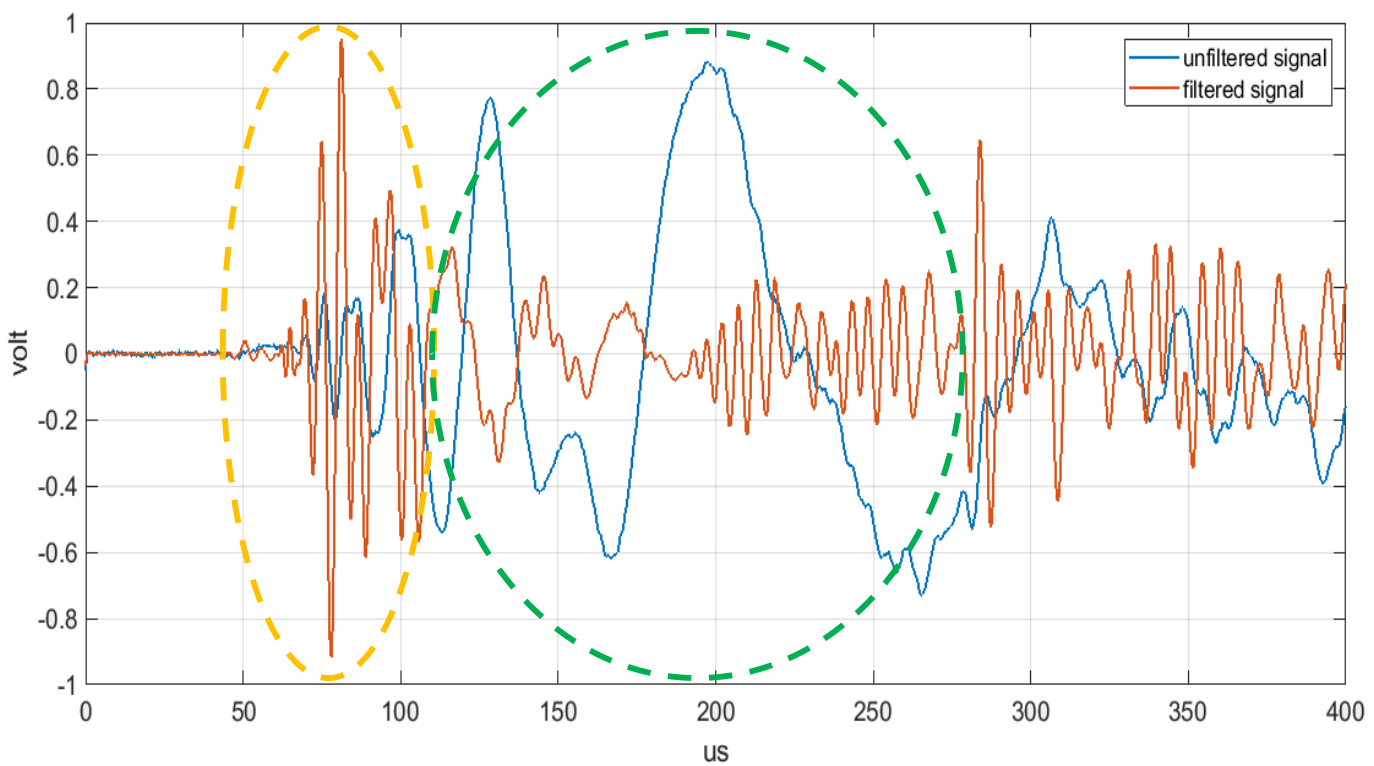


Figure 3 Ultrasonic signals generated by a low-velocity impact (about 3m/s) in blue colour, and the same signal filtered by an analog low-pass filter with a cut-off frequency of 400kHz in red colour. The dotted green circle represents the portion of the signal relative to the A_0 mode; the dotted yellow circle represents the portion of the signal relative to the S_0 mode.

From the analysis of Figure 3 it is apparent that the fast propagation mode S_0 become comparable in amplitude with the A_0 mode only after filtering the ultrasonic propagating signal generated by the impact. The possibility to process the fast S_0 mode instead of the slower A_0 mode, is often the best signal processing design strategy, because this early arrival time signal is less affected by overlapping of the multiple reflections from the structure edges [28]; moreover, the impact signal detection and positioning is even more complicated in large structures for the higher attenuation and the mode conversions after the propagation on areas with different thicknesses. The topics briefly reviewed in this section remarks the importance of the understanding the physical background for designing sensors and the analog front-end to simplify and make reliable the information extraction from the signal.

2.3 - Signal processing techniques for dispersion and environmental factors compensation.

From the preliminary considerations in the Introduction, we can remark that the rapid evolution towards integrated-SHM (ISHM) systems operating in different environmental conditions follows a different path than common AE and NDT techniques, that use volumetric longitudinal or transverse ultrasonic waves with piezoelectric transducers connected to portable instruments and the region of interest (ROI) manually scanned of by a trained operator [29]; main differences are found for the signal processing adopted both for passive and active mode operation of the SHM system.

The analysis of information gathered by a sensors layout due to the interaction between the UGW dispersive modes and the various types of structures is certainly a challenging aspect from the point of view of signal processing techniques that are based in a widespread way on the Continuous Wavelet Transform (CWT) or the Short Time Fourier transform (STFT). CWT decomposes a time domain signal into components corresponding to a frequency band. Each of these components contains a further temporal discretization. The resolution of the temporal discretization varies with each frequency component resulting in a multi-resolution temporal frequency analysis.

Since the modes S_0 and A_0 propagate with different amplitudes in the useful band and with different propagation speeds (see Figure 2), the CWT allows a representation capable of separating the two contributions in different instants of time. One of the limitations of the CWT is the compromise between resolution in frequency and in time and moreover the calculation algorithm requires considerable computational resources, not always available within a sensor node. Alternatively, the simplest form is represented by the STFT, which however does not have the possibility to implement the multi-resolution functionality in the time / frequency domain. For example, the separation of the two modes S_0 and A_0 by CWT o STFT is relevant for the evaluation of the DToAs for

low and high velocity impacts, as we will describe in section 2.2. However, simple analysis with CWT or STFT may still be too restrictive in the presence of structures with inserts, reinforcement elements and therefore recently several methods have been proposed to overcome this problem, such as reported in [30–32]. Another important method introduced in [33] to compensate for the dispersion and alleviate the complexity of Lamb wave signal interpretation, is the well-known time-reversal approach; this approach was adopted by Zeng et al [47]. UGWs used in active mode for damage assessment have a great sensitivity to detect internal damage into the structure and this is one of the main reasons of successful application of this NDT technique. The detection is often implemented on a data driven approach, where received UGWs from a sensor layout is compared with a baseline of data acquired with a pristine structure. This approach is rather simple to be implemented also in sensors with on board embedded processing, but it suffers from the sensitivity to environmental and operational conditions, mainly temperature variations. Recently, Mariani et al [34,35] have proposed a method for the compensation of this detrimental phenomenon. For the electro-mechanical-impedance (EMI) method, the temperature compensation was achieved with some benefits by using artificial neural network (ANN) as reported by Sepehry et al [36].

2.4 - Advanced methods for impact detection and localization.

In general impacts on a thin planar structure generate guided waves modes that can propagate away from the impact point. The localization of the impact point is commonly achieved by adopting a triangulation algorithm with at least three passive ultrasonic sensors deployed on the planar structure. The accuracy of the impact point estimation depends on the estimates of the guided modes velocity and the measured differential time of arrival (DToA) among the sensors [37]. Recently several papers have been published to improve the reliability and accuracy of impacts on complex structures other than from the simple panels often used by researchers in laboratory for calibration and performance assessment of a SHM system. The Akaike Information Criterion (AIC) criterion for the accurate estimation of DToA has been demonstrated by De Simone et al [38]. Further research work has consolidated the investigation of the advantages of AIC and a modified version for impact monitoring has been recently proposed by Seno et al [39]. In the latter work an ANN was trained for automatic classification of defects in composite materials tested in laboratory and in simulated operational conditions. As already reported in the Introduction an extensive review of AE physical parameters for SHM systems is reported by Ono in [15]. The characteristic of UGW generated by impacts have been outlined in sections 2.1 and 2.2. Such guided wave modes propagating into the planar structure mix-up due to the phase velocity dispersion and in addition the reflection phenomenon from the edge or from inserts or stiffening material or defects [40]. Moreover, mode conversion can occur when the ultrasonic guided waves travel across a discontinuity of acoustic properties in the planar structure, for example a change in thickness or material composition. In general, the wave shape of the impact generated UGW is complex but a list of features supported by theoretical modelling developed by Hakoda et al [41] based on the phase velocity analysis can be derived. It is worth to observe that the propagation velocity analysis in general is more complex for composite structure

respect to the simple case shown in Figure 2; even the example of time domain signals generated on an aluminium plate reported in Figure 3 is a simplified scenario respect to real-life cases. In the following we report two main considerations that are starting guidelines for the impact signals processing:

- 1) the early part of the signal consists of the fast phase velocity modes, typically the S_0 mode in the low frequency range below the cut off $frequency \times thickness$ product (e.g., equal to 1.5 MHz \times mm in *Figure 2*).
- 2) in the later part of the signal the contribution comes from slower modes that show also dispersion effect as for the A_0 mode [42] or signals that travelled along longer paths or multiple reflections.

We can observe that S_0 mode being faster it is less prone to be hidden by the other signals but has a lower amplitude as its attenuation is higher than A_0 mode; the higher velocity of this mode implies also that the error on its DToA estimation causes higher spatial errors in the triangulation algorithms or any other positioning method based on DToA [43–45]. The theory of UGW in a plate like structure considers also other type of waves than Symmetrical and Antisymmetrical Lamb wave modes: the shear horizontal (SH) mode. This is a non-dispersive mode and piezoelectric sensors/transducers can be designed to convert this wave type into voltage signals. Ren and Lissenden [46] have demonstrated capability of sensing also Lamb waves that are of interest for impact detection in passive mode. Altammar et al [47] studied the actuation and reception of shear modes by exploiting the d_{35} piezoelectric coefficient of lead zirconate titanate (PZT) sensors embedded in a laminate structure.

d_{35} PZT is a class of PZT piezoelectric transducers that when polarized along their thickness, they induce shear strain in the piezoelectric material. It is interesting to observe that the shear

deformation has a stronger coupling coefficient (d_{35}) than the common d_{33} or d_{31} , indicating d_{35} PZTs have stronger electromechanical coupling for sensing and actuation.

In the final part of this section, we review the advancements on signal processing techniques for anisotropic plate-like material. Anysotropic characteristics of composite structure require the adaptation of impact positioning algorithm developed for isotropic plate like materials. The early research on signal processing techniques for isotropic metallic plates and anisotropic composites can be found in [21,45,48,49]. More recently the signal processing techniques have been progressed to account for the UGW dispersion (see section 2.1) and anisotropy of different type of composites like unidirectional, quasi-isotropic composite fibre reinforce polymer (CFRP) and honeycomb, of interest for aerospace industry [38,45,50–52]. An early work of Scholey and Wilcox in 2010 [53], addressed the problem of impact detection on 3D structures and recently Moron et al in 2015 [54]. Lanza di Scalea et al. published a work [55] for impact monitoring in complex composite material structure with an algorithm based on the rosette sensor configuration; this model-based approach could solve the problem of variation of phase velocity along different direction of a composite material.

3. Sensors and transducers for impact monitoring

Piezoelectric sensors are common devices for the passive detection of impacts on the structure [56]. However, an SHM system can also operate in active mode with piezoelectric transducers for generating UGW for damage evaluation because of impact events. In this way there is an interest to have a dual use of the transducers both for passive and active operation with an advantage on the

reduction of system complexity. In this section we will revise the main characteristic of sensors and some considerations how to use transducers in passive mode are reported.

3.1 Single element piezoelectric sensors for impact detection and emerging/new sensing materials.

The piezoelectric sensors commonly used for reproducing the impact stress waves in passive mode are typically based on PZT, BaTiO₃ or polyvinylidene fluoride (PVDF) piezoelectric materials [7,22,23,37,57–61]. According to the choice of piezoelectric material, the sensor design or selection is completed by the definition of the fabrication technology and the dimension/shape that must accomplish to several system level target parameters such as:

1. Bandwidth
2. Sensitivity /Gain /signal to noise ratio (SNR)
3. Input Impedance
4. Input signal dynamic
5. Temperature range
6. Mechanical features: Stress / Strain / Brittleness / Flexible /Stretchable
7. Bonding / Embedding
8. Electrical connection/wiring
9. Cost

Typically, single element sensors have planar dimensions in the order of several millimeters and operate in non-resonant mode; these conditions lead to an almost isotropic (omnidirectional) sensitivity to UGW and broadband frequency response (e.g. 20 kHz – 1MHz), so that are versatile sensors for many applications as they cover a large range of the fxd product of the phase velocity

diagram (see section 2.1). On the contrary these broadband sensors are not UGW mode selective and as pointed out in section 2, the overlapping of different modes requires clever signal processing to extract information on impact position.

For example, a comparison of different type of sensors can be made observing three different and common sensors technology for UGW detection (see Figure 4). By comparison, the electrical, mechanical, and piezoelectric characteristics of these three types of materials it is quite straightforward that for each application we can select the most appropriate sensor technology.

The characteristics of these three sensors shown in Figure 4 are reported in Table 1.

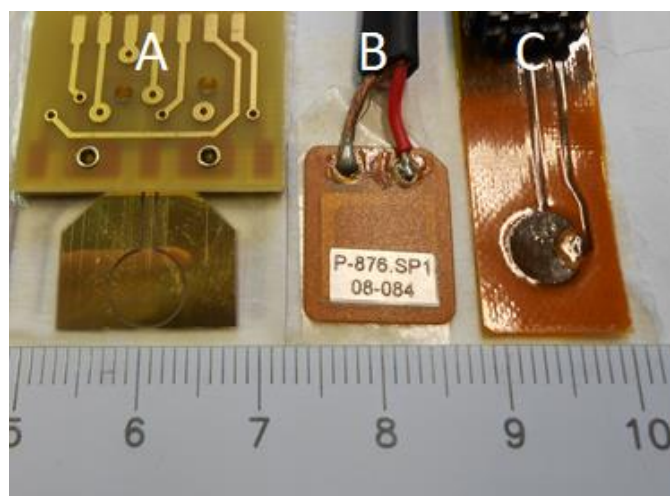


Figure 4 Example of three different type of piezoelectric sensor for SHM: (A) circular PVDF sensor made with bioriented PVDF film furnished by Precision Acoustics, (B) BaTiO₃ piezocomposite, model DuraAct produced by Physik Instrumente, (C) PWAS, model SML-SP produced by Acellent.

TABLE 1 CHARACTERISTICS OF SINGLE ELEMENT PIEZOELECTRIC SENSORS.

Type	A	B	C
Model	Circular_PVDF	P-876.SP1 DuraAct	SML-SP-1/4-0
Manufacturer	By authors (Precision Acoustics material)	Physik Instrumente	Acellent
Capacitance	86 pF	8 nF +/-20%	1.1 nF
Thickness piezoelectric element[μm]	110	200	140

Material	Piezo-polymer	Piezo-ceramic	Piezo-ceramic
Shape	Circular	Rectangular	Circular
Dimensions [mm]	Diameter 6.5	16x13	6
Operation temperature Range	-80 °C, +50 °C	-20 °C, +150 °C	-40°C, +105 °C
Acoustic Impedance [MRayl]	2.7	30	33

By the analysis of Table 1 for three sensors having comparable area, it can be pointed out the difference in capacitance that is a relevant parameters for the electronic design (see Section 4) and the acoustic properties made clear the different performance for the acoustic matching with different materials like metal or CFRP that influence the sensor sensitivity; while piezoceramic material are well matched with metals, piezocomposite and piezopolymers are better suited for plastic composites.

In the literature are reported several types of commercial and customized sensors that can be compared according to the list of nine points reported above. For example, Wu et al. [59] compared the commercial Accelent Smart Layer® sensors arranged in a SMART Layer (SL) with PZT flexible ultrasonic transducers (FUT) fabricated with sol-gel process in order to achieve a large bandwidth for inspection of materials with large thickness with surface waves (3-6MHz) or for NDI of small kxd products of laminate materials with UGW (300-600 kHz). An interesting publication about the state of art for in service application of commercial transducers for SHM in aerostructures is available [62].

Qi et al. [63] compared PVDF film and PZT patch sensors for impact monitoring of low velocity impacts in smart aggregates and the conclusive remarks is that there are relative merits for both materials. Jia [64] analyzed the dynamic response of embedded PVDF sensors at different impact velocity (see section 2.2).

Recently the research is moving toward new sensors and there are important novelties in the research of functional materials with enhanced piezoelectric properties: an example published recently by Han et al [65] is the development of highly sensitive impact sensor based on a PVDF-TrFE/Nano-ZnO composite thin film. The percentage of doping of PVDF TrFe Copolymer with ZnO increases the sensor sensitivity and the dielectric constant. That paper reports also preliminary results on signal acquisition for different impacts. Another approach was proposed by Capsal et al [66] by the technology development of a flexible, light weight and low-cost electroactive coating obtained by the dispersion of BaTiO₃ submicron particles on a in a polyurethane matrix; the experimental set up was demonstrated to detect impacts on an aircraft structure in real time. Finally, a recent study on piezoresistive properties of silicon carbide (SiC) has been published by Kwon et al [67]: a SiC fibre sensor network has been embedded in a composite structure for low-velocity impact localization on a composite structure. The SiC fibres have potential to reduce the mechanical discontinuities introduced by the sensing elements that is a critical point for the embedment of many types of piezoelectric elements. Another innovative approach introduced in [68] is the adoption of nanotechnologies for embedding carbon nanotubes (CNT) into composite materials and the analysis of electrical resistance variation for high and low energy impacts is shown. The introduction of new materials for sensing impacts and damage monitoring is a new fertile field for the research and the advantages and disadvantages respect to common piezoelectric sensors will be clear when such devices will be more mature by moving from laboratory to real-field tests.

3.2 Multifunctional sensors based on piezopolymer film material.

The possibility of using the same device operating in passive mode for impact monitoring and for damage detection and localization in active mode, is an important advantage to simplify the SHM system complexity. Moreover, added sensing capabilities to the same device as temperature or strain measurements, lead to a new type of devices that are called “multifunctional” sensors. For example, the data obtained from these devices are usefully processed by clever algorithms to compensate for variation of the UGW propagation and physical sensor properties due to thermal drift (see section 2.3). In addition, the UGW mode selection for the damage evaluation is another useful requirement to have in a transducer. In this section we will explore the concept of a multifunctional sensor based on interdigital transducers (IDTs). IDTs for guided Lamb wave offer the advantage over single element transducers (see Figure 4) of the selection of Lamb wave mode for a given material by the definition of the kxd product (see Figure 2); in this regard they can be considered as narrow band devices. IDTs for guided Lamb wave applications are created by a sheet (or thin plate) of piezoelectric material equipped with electrodes on the opposite surfaces: at least one side must host two sets of interleaved comb electrodes with separate connections, while the other may present a ground plane, another pattern of electrodes. A common exploded view of an IDT is shown in Figure 5, where the geometrical parameters are also defined. The transducer has one side coupled to the ultrasonic wave guiding medium (a plate-like structure). The two sets of comb electrodes are generally assumed to operate with 180° -out-of-phase signals (both in transmission and reception), such that the transducer provides geometrical wavelength selectivity when attached to the surface of a plate-like waveguide. The IDTs made by piezopolymer film like PVDF, have a unique advantage respect to ceramic of flexibility and conformability to non-planar

surfaces but, according to Table 1, their limits on the temperature range as well as different sensitivity must be well understood and investigation results are reported in the following sections.

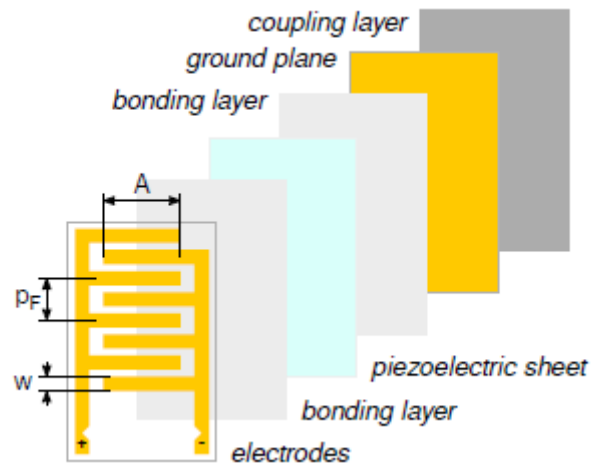


Figure 5 - Exploded view of an interdigital transducer assembly. "A" is the length of the electrodes (fingers), "p_F" is the finger pitch and "w" is the finger width.

IDTs developed by our group present a difference with those published by other research teams in that they are manufactured via laser etching, starting from metal-coated—usually with Pt-Au, or Cr-Au alloys—poled PVDF sheets. Since PVDF is mostly transparent to the laser beam, it does not heat up considerably during the etching process, and the laser passes through the polymer etching the back-side metallization as well. Therefore, the process results in having an identical electrode pattern on both sides of the PVDF.

The possibility to ablate with a quick process (tenth of seconds) an arbitrary pattern on the metal coating of the piezo-polymer film by laser ablation, constituted an enabling technology for including different sensing elements on the same film and reduce the production costs of multifunctional sensors.

For this purpose, two additional sensory patterns have been etched alongside the IDT electrodes on the same piezo-polymer film device: a 1/4" circular element (impact passive sensor), and a

resistive temperature device (RTD). The picture reported in Figure 6 illustrates the three patterns for the multifunctional sensor alongside the dimensional drawing.

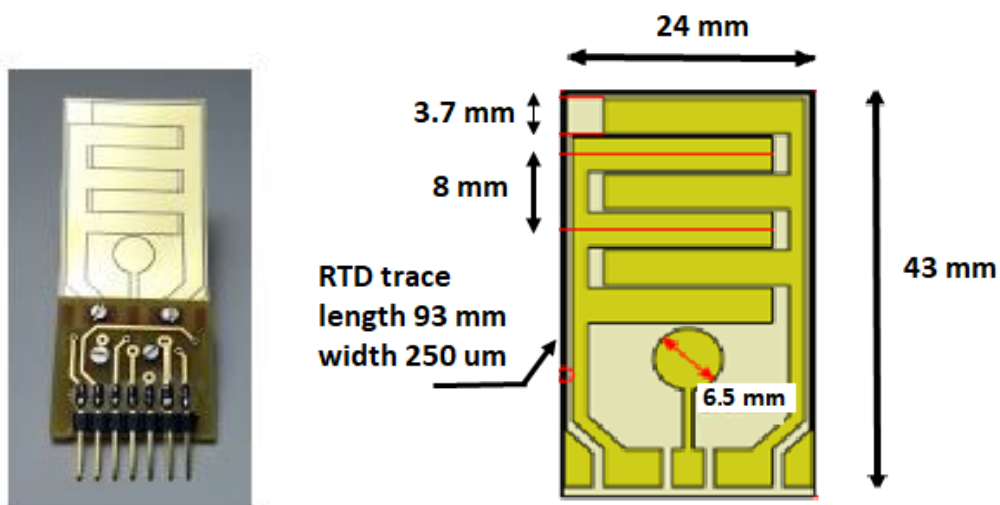


Figure 6 (Right) Multifunctional sensor: IDT for active mode with finger pitch 8mm, circular sensor with diameter 6.5mm for impact sensing, RTD for temperature monitoring with length (43+43+24) mm=110mm; (Left) dimensional drawing of the fabricated device by laser ablation of the metallization.

3.3 Comparison of piezoelectric PVDF and PZT sensors sensitivity for impact detection.

In the previous section is reported the design and fabrication of a circular sensor integrated in the same IDT device with the aim to capture impact generated Lamb wave signals propagating from any direction respect to the sensor centre. Some companies have specialized in providing patch piezoelectric sensors with characteristics suitable for acoustic source localization, and off the shelf devices are available from Acellent and Physik Instrumente. Specifically, in our design the circular PVDF sensor has a diameter of 6.5 mm, similar to Acellent's SML-SP-1/4-PZT sensor (1/4", or 6.35 mm) (see Figure 4).

The sensitivity of the circular piezoelectric element as a receiver were assessed by comparing it to a PZT device of similar active area (see Figure 4), the Physik Instrumente P-876.SP1. These two sensors were taped side-by-side to an aluminium plate 1.2 mm thick, with a third transducer used

as transmitter and placed at distance of 200mm from both. A Morlet wavelet centred at 250 kHz was transmitted and received using the same pre-amplifier for both sensors: an instrumentation amplifier (INA) providing a voltage gain of 78 dB at 250kHz. The excitation wavelet and the acquired traces are plotted in Figure 7(a) and 7(b) respectively.

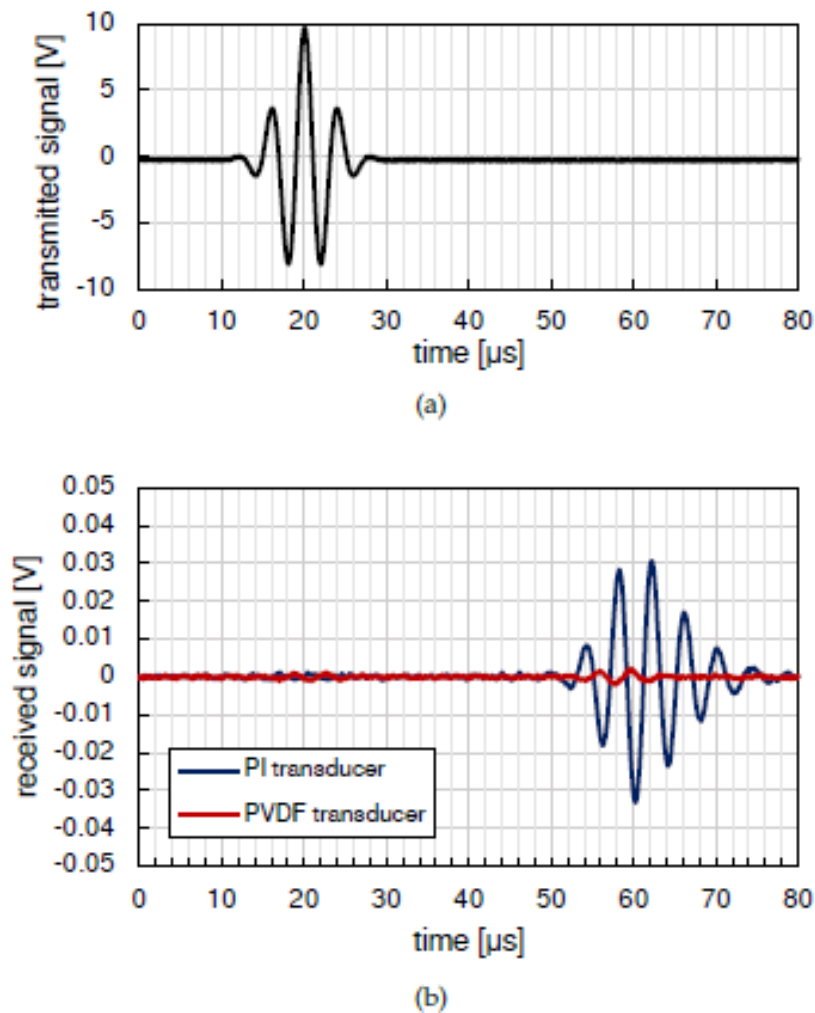


Figure 7 Experimental sensitivity comparison of the circular element with a commercial PZT sensor of same class: (a) transmitted Morlet with central frequency 250 kHz; (b) signals received from the two sensors (PI blue colour and PVDF red colour).

The plot shows that, as expected from the piezoelectric properties of the materials, the circular element sensitivity is lower than the PZT device. Such a wide difference, however, may not be a problem in impact detection applications, where signals tend to be rather large as reported in [64] for different impact velocities. In some cases, the large input voltage at the preamplifier input

exceeds the rail-to-rail input and saturate the output with consequent loss of information of the impact event. In conclusion the different sensitivity of the two piezoelectric materials is not a limiting factor for the choice between the two. There are other differences between that must be considered for the choice of the sensor technology as temperature. In the following section we analyse the operating temperature range of PVDF piezo films, being limited respect piezoceramic and piezocomposites (see Table 1).

3.4 Operating temperature range estimation of piezopolymer sensors.

In this section we report the assessment of the temperature operational limits of the PVDF material for considering their use in harsh environments (e.g. aerospace). The authors carried out some measurements at cryogenic temperatures (up to -80°C) and at high temperatures (up to +50°C) using a piezopolymer sensor pair in pitch-catch mode, realized with P(VDF-TrFE) copolymer film. A series of cryogenic treatment tests of the P(VDF-TrFE) film sensors were conducted at the following temperatures: -20°C, -40°C, -60°C, -80°C.

The conditioning procedure consisted of the following steps:

- Inserting the sample into the steel tube housing (see Figure 8 left).
- Immersion of the sample in the cryogenic chamber remaining above the liquid nitrogen level.
- Time to reach the desired temperature (from 20 to 40 min).
- Test duration time 20 min.
- Sample recovery time up to room temperature 15-30min.
- Test the sample on reference aluminum laminate supplied by TAS-I (see Figure 8 right), using sample IDT #1 as transmitter and IDT #2 as receiver.

At first, we attached the sensor pair (IDT #1 and IDT #2) to an aluminium laminate with a bi-adhesive tape at a certain distance in a pitch-catch configuration and we recorded the ultrasonic signal collected to the receiver transducer before the treatment. Then we removed the receiver and we treated it at the cryogenic temperatures. After the treatment we repositioned the receiver on the plate and we recorded again the signal received. Comparing the collected signal to the receiver after the temperature treatments, we pointed out that no variation in terms of signal amplitude has been recorded for all cryogenic testing temperatures.

Another test has been carried out at temperatures up to +50°C by heating a pair of sensors attached with a bi-adhesive tape (furnished by Eurocel - SICAD group) to an aluminium plate in a climatic chamber for about one hour. The detailed description of the testing procedure is reported in the following:

- Setting of the desired temperature by remote programming of the air conditioning system with Peltier cell.
- Wait for the time to reach the desired temperature equal to 15 min.
- Test duration time 20 min.
- Acquisition of the signal on the IDT # 1 sensor, using the IDT # 2 as transmitter.

Then we recorded the ultrasonic signal collected to the receiver transducer before the treatment and we recorded the same signal after reaching the temperature of +50°C. Again, comparing the collected signal to the receiver before and after the temperatures' treatment we pointed out that no variation in terms of signal amplitude has been recorded. After these tests we concluded that this type of material could be used certainly down to -80°C and up to +50°C without degradation in its piezoelectric properties. The thermal properties are also relevant for the permanent bonding of

piezopolymer sensors on the structure by epoxies that often require curing temperature between up to +60°C.



Figure 8 (Left) Piezopolymer sensors introduced in the cryogenic chamber. (Right) Experimental set up with two piezopolymer transducers in pitch-catch configuration for comparison of performance before and after the cryogenic treatment.

3.5 Advanced technologies for Piezoelectric Sensors in SHM systems

The main piezoelectric materials analysed in section 3.1, have been used to design different type of sensors and transducers in the last two decades with the scope to be integrated with the target structure. In this section we will review the developments of more advanced sensors and transducers designed for achieving different characteristics:

- embedded sensors with the structure.
- Lamb wave mode selection,
- array configuration

Sensors and transducers are often combined for passive and active mode operation. Lehman et al [42] reported the advantages of a piezocomposite transducer made by PZT fibers demonstrating the possibility to integrate such transducer in an aircraft wing. This early paper introduced the concept of sensor node with electronic integration and connection to a base station; a graphical description of this system configuration is shown in Figure 9. The same paper also addressed the advantages and disadvantages of the removable sensors with adhesive tape bonding respect to permanently bonded sensors in composite structures; this problem is often found when a prototype system as to be tested in laboratory before to final testing on the final structure. It is worth to note that this type of sensor was also tested for impact detection based on the observation of a dispersive A_0 mode generated in a CFRP plate.

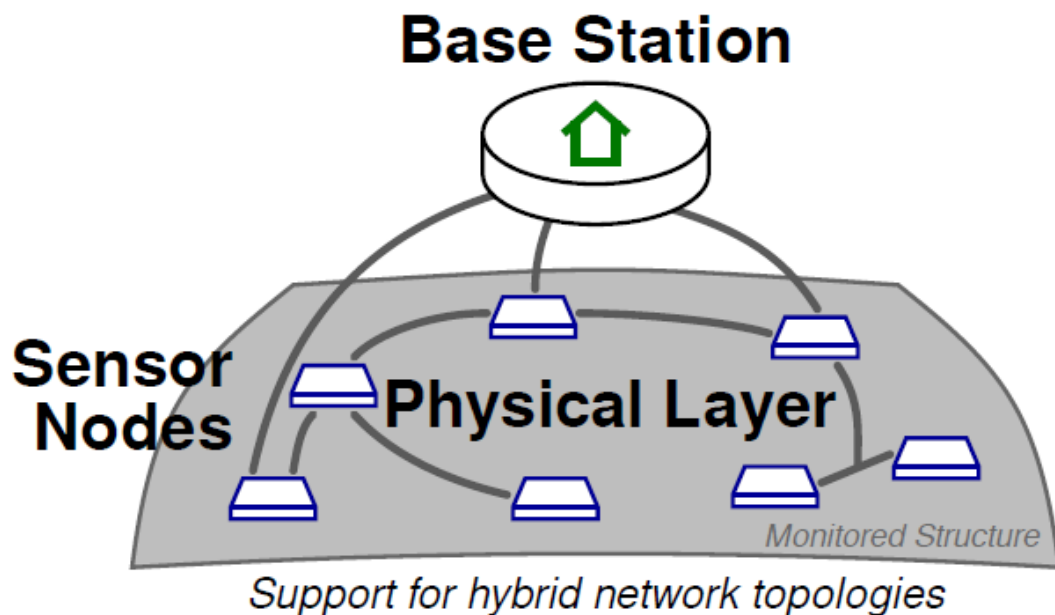


Figure 9. Graphical representation of a wired sensor network for SHM.

3.5.1 Sensors embedding

Another issue for sensors is the embedding in the structure to ensure durability for service in harsh environmental conditions. An example of the embedding PVDF IDTs was also carried out for

composite CRFP materials by Bellan et al [69] but no easy solution for connections and wiring of the piezoelectric film was provided. Following these early works, an innovative approach based on bioinspired sensors, was proposed by Ghoshal et al [70] with a ribbon of PZT element array. Recently, the concept of “smart-skin” (SS) of bioinspired embedded sensors was developed with several advantages on the installation and the simplified task for signal acquisition and processing [71]. Another interesting approach for “aircraft smart composite skin” (ASCS) was proposed in [72] with the investigation of efficient ways to connect in series and/or parallel a large number of PZT sensors with front end electronics; a signal processing strategy to convert analog information to digital sequences was also a main result towards to simplify the embedded signal processing.

Another innovation on sensor technology was stimulated by the installation of stretchable sensor networks on structures subjected by large mechanical deformation/strain under mechanical loading (e.g. Composite Overwrapped Pressure Vessel (COPV)) [73]. The concept of flexible sensors has been further investigated in [74] with “bioinspired stretchable sensors” (BSS) with multifunctional capabilities; a screen-printed PZT technology on a substrate flexible electronics is envisaged as enabling technology for integration of SHM system with the monitored mechanical component. Another interesting review of novel EMI method for integrating piezoelectric sensors in a concrete structure or in a transportation vehicle is reported in [75]; these two different target installations both imply the operation in harsh environment; therefore, the sensor protection by additional layer or by embedding is a key point to ensure the durability of the sensors and the system functionality. Another recent work regarding the application of stretchable sensors for AE location is proposed in

by Hu et al [76] where an array of 10x10 PZT elements encapsulated in silicon elastomer layers have been developed and preliminary tests on non-planar 3D surfaces are reported.

3.5.2 Lamb wave mode selection

For the Lamb wave mode selection, a suitable transducer structure is the IDT as reported in section 3.2. PVDF IDT type of transducers were first proposed by Monkhouse et al [57] to generate Lamb waves in structure and following works by Capineri et al [72] and Mamishev et al [73] have developed the fabrication technology, while the analysis of electrodes shape for tunable transducers is reported by Lissenden [46]. The latter characteristic is fundamental for the mode selection that in many cases simplifies the interpretation of the signal information. An extensive review of the IDT technology is provided by Mańka et al. [77], Stepinksy et al [61] for tunable IDT realized with piezoelectric micro-fibre-composites (MFCs). Arrays of IDT employed in passive mode for impact detection have been experimented in an integrated SHM monitoring system for pressurized tanks by Bulletti et al [60] but the location accuracy needed was limited by the anisotropic sensitivity response of the IDT as demonstrated by Lugostova et al [78]. Moreover, the evolution of IDT used in both passive and active mode, is the array configuration where each pair of finger electrodes can be connected independently to a channel of the AFE, which allows to drive or receive signals with different time delay and gain to improve the Lamb mode selection and apply signal apodization, as shown by Bulletti et al [79].

Because the anisotropic response of the IDTs is a limiting factor when used as impact sensors, several works have investigated this design issue from the theoretical point of view Wilcox et al [80], Wang et al [81] and by experimental works, Mańka et al [82], Lugostova et al [78,83]. As shown in

section 3.4, the multifunctional sensor solution with a circular piezoelectric element included in the same device with an IDT and a RTD sensor can overcome the problem of isotropic and broadband impact sensing without adding complexity and cost to the system (see Giannelli et al [84]). In this regard, a complete review of the SHM sensors technologies and systems is recently published by Qing et al [37] where a network of multifunctional sensors for environmental adaptivity is proposed: EMI, UGW, RTD and strain data can be used and correlated to minimize the influence of variable operating conditions.

The concept of Ultrasonic Guided Mode (UGM) selection by an IDT tunable transducer have been expanded by studying different electrodes geometries like the spiral transducer developed by De Marchi et al. [85]: in that paper the synthesis of directivity is presented and can be usefully adopted for the definition of the sensors layout and number of sensors/transducers to be installed on a defined structure; moreover that paper indicates also a suitable signal processing strategy based on DTOA information for considering the spiral based patterned geometry. Other type of electrode patterning has been studied as the annular shaped IDT designed for SHM application published by Koduru et al [86] and Gao et al [87]. This solution has been recently implemented with screen printed technology by Salowitz et al [88].

3.5.3 Array configuration

In general sensor network are installed on the structure to have an optimal area coverage. An alternative solution is the installation of an array of transducers for implementing the scanning of the area by electronic beam steering in transmission and receiving mode. The latter is also of interests for the implementation of algorithms for the estimation of the direction of arrival of a Lamb wave

generated by an acoustic source. The programmable beam direction of a transducer emission and reception can be obtained by the well-known phased array solution common in the NDT and medical ultrasound echographic instruments, equipped with integrated analog-digital electronics to achieve a real-time beam steering. Generally high spatial resolution imaging is obtained for the ROI selected on a portion of the plate-like structures, that must be reachable by a line of sight from the phased array without obstacles (inserts, stiffeners, bolts) in between. The SHM based on phased array implies higher cost, higher power consumption and is not scalable with the dimensions and shape of the structure. There are important developments recently published by Giurgiutiu et al [89] with arrays based on piezoelectric wafer active sensors (PWAS) and more recently by Ren et al [46,90], with 16 elements PVDF arrays operating in a broad bandwidth (0.2-3MHz). An example of an embedded instrument capable to program a phased array by remote connection is the Pamela project developed by Aranguren et al [91]: an embedded electronic instrument with Field Programmable Gate Array (FPGA) can be programmed for specific signal processing of data acquired by a 16 piezoelectric element phased array.

4. Influence of front-end electronics on impact detection and localization

In the previous sections we have described the importance of the choice for the sensor technology and configuration for passive impact sensing while in this section we will address and explain other important issues for the analog front-end design: impedance matching, input signal dynamic, bandwidth, distortion and power supply. The role of electrical impedance matching is crucial for SHM integrated system design as the operating bandwidth is continuously increasing and different type of AE sensors are in use; for this aim a recent paper has been published by Rathod et al [92]. Poor

electronic design lead to a loss of information on the impact event as reported by Qing [37], where several approaches are presented to process the signals generated by a set of sensors; other relevant works for the electronic design developments of sensors network are the Match-x project [93] and the work of Ferin [94]. A useful reference paper for AFE designers is published by Beatie [95], where an analysis of important electronics characteristics of the AFE and their influence on the overall impact detection performance is reported. Today Analog to Digital Converters (ADCs) can acquire at a sampling frequency (F_{samp}) of 50 MHz with 16-bit resolution and at low power with 3.3V voltage power supply. Such resolution implies a 90dB dynamic at the ADC. This large input signal dynamic range is useful to preserve signal integrity when both low and high velocity impacts must be monitored. The choice of the sampling frequency is important to avoid oversampling nuisance in automatic signal processing schemes and high data rate transmission from sensor node as noticed in the work of Ebrahimkhanlou et al [96]. Typically for a broadband SHM system, it is required a maximum analog bandwidth of 1MHz which lead to a minimum frequency sampling of 5MHz considering a 5-fold factor; at this sampling rate the new ADC technologies have a low power consumption.

4.1 Programmable single channel front end electronics for signal conditioning

In this section we will explain the advantages of designing or using a programmable electronic for interfacing piezoelectric sensors with different impedance and sensitivity and we will review the main design concepts. In Figure 10 are shown the main electronic components of a programmable single channel AFE and we include a numerical example for the evaluation of performance; the list of the main components is reported as follows:

- 1) A low noise amplifier (LNA) with fixed open loop voltage gain (typically 10dB) and programmable feed-back impedance to match the sensor impedance bandwidth equal of larger than the sensor (e.g., 50kHz- 1MHz). For example, we can assume a Noise Figure (NF) better than 5 dB, input equivalent noise density $0.6 \text{ nV}/\sqrt{\text{Hz}}$.
- 2) A programmable Variable Gain Amplifier (VGA) for adjusting the signal amplitude to the input voltage rail of the ADC (e.g., selectable gain -10dB, +30 dB).
- 3) A passive anti-aliasing filter (AAF) with attenuation rate depending on the filter order (typically 6dB) and cut-off frequency $f_{\text{cut-off}}$ equal to the higher spectral component of the input signal.
- 4) An ADC with sampling frequency F_s selected according to Nyquist criterion and higher 5-20 times the $f_{\text{cut-off}}$. The ADC should be selected with low equivalent noise floor.

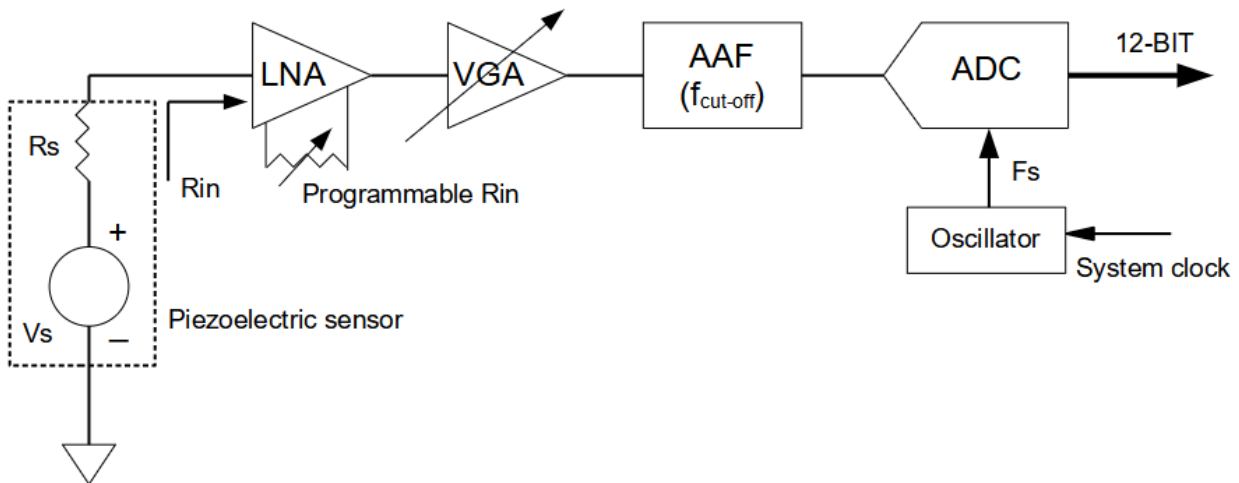


Figure 10 - Programmable single channel AFE for signal conditioning of piezoelectric sensor.

By a numerical example is here illustrated the intrinsic noise performance for this chain that allows a programmable gain of the VGA to adjust for different input signal amplitudes. The total voltage gain can be calculated with the reference component values and the max VGA gain of 30 dB:

$$\text{AvTOT(dB)} = \text{Av(LNA)} + \text{Av(VGA)} - \text{Av(AAF)} = 10 + 30 - 6 = 34 \text{ dB or about } 50 \text{ V/V} \quad (2)$$

For this value considering an input dynamic of 3V dictated by the rail of power supply voltage of the ADC, we can manage a signal input generated by the sensor with voltage Vs:

$$Vs = 3V/50 = 60 \text{ mV} \quad (3)$$

Assuming an equivalent noise density for a 16bit ADC of $Vn(\text{ADC}) = 30 \text{ nV}/\sqrt{\text{Hz}}$, we can calculate the equivalent input noise for the maximum $Av_{\text{TOT}(\text{dB})}$ that is:

$$Vn_{\text{in}}(\text{ADC}) = Vn(\text{ADC}) / Av_{\text{TOT}(\text{dB})} = 30 \text{ nV}/\sqrt{\text{Hz}} / 50 = 0.59 \text{ nV}/\sqrt{\text{Hz}} \quad (4)$$

This equivalent input noise should be equal or smaller than the intrinsic input noise of the LNA and in this case the criterion is satisfied being $0.6 \text{ nV}/\sqrt{\text{Hz}}$.

The setting of the max VGA gain can be changed to adapt the amplification of signals generated by higher energy impact to avoid saturation, for example a $Vs = 200 \text{ mV}$. $Av_{\text{TOT}(\text{dB})}$ can be now recalculated by (2) for this case:

$$Av_{\text{TOT}(\text{dB})} = 3V/0.2V = 15 \text{ V/V} \quad (5)$$

According to (3) the $Vn_{\text{in}}(\text{ADC})$ increases to the new value:

$$Vn_{\text{in}}(\text{ADC}) = Vn(\text{ADC}) / Av_{\text{TOT}(\text{dB})} = 30 \text{ nV}/\sqrt{\text{Hz}} / 15 = 2 \text{ nV}/\sqrt{\text{Hz}} \quad (6)$$

The new operating condition shows a decreased SNR performance being the ADC input noise exceeding the LNA noise. Assuming the worst case of the latter example for a bandwidth of $B = 1 \text{ MHz}$, the equivalent input noise voltage is:

$$Vn_{\text{in_equivalent}}(B = 1 \text{ MHz}) = Vn_{\text{in}}(\text{ADC}) \times B = 2 \text{ nV}/\sqrt{\text{Hz}} \times \sqrt{1 \text{ MHz}} = 2 \text{ mV} \quad (7)$$

This value needs to be compared with the lower amplitude of the Lamb wave mode signal that can be received for a given sensor sensitivity, especially if a signal processing scheme is based on a threshold method. Often low impact velocity impacts generate fast S_0 mode signals in order of tens of microvolts and in that case the AAF must be designed to the minimum bandwidth requires and the voltage gain set to maximum available in the chain.

This analysis explained by relationships (1)-(7) is useful to demonstrate one of the trade-offs for the design of the AFE when the input signal has large amplitude variations. A good example of this situation is the signal conditioning of an impact signal described in Section 3.2, where the generated S_0 leads the slower A_0 and the amplitude ratio between the two signals can be 10-fold factor.

These problems (SNR, gain setting, dynamic) are partially overcome today by using component of the shelf (COTS) integrated circuit for AFE, but their characteristics are often optimized for the NDT and medical ultrasound sensors, while for the SHM the input voltage levels and bandwidth differ from those fields. Moreover, the integrated devices that include ADC have steady state power consumption compatible with power supply unit for electronics in a base station (see Figure 8) but such power consumptions are rather demanding when the electronic front end is close to the sensor, as for the solution of a battery operated node for a sensor network. Yun in his master thesis [97] have proposed an electronic solution for impact detection with nodes implementing EMI method where the impact signal triggers a low power comparator that switch on the power supply of the rest of the electronics for acquiring the signal over a defined amount of time. This type of solution alleviates the problem of power supply for continuous monitoring. Thomas et al [98] demonstrated

that a coverage with rings of AE sensors installed on composite tube can produce high quality images of damage by an EMI tomographic method.

Another electronic design issue is the pick-up of environmental noise when broadband sensors are adopted. The extrinsic electromagnetic noise picked up by the wiring of the sensor to the AFE, is an additional source of SNR deterioration unless bulk coaxial cables are used. A quite robust solution that mitigates the common mode noise is the differential connection of the sensors, but this implies the design of special differential amplifiers with high common mode rejection ratio (CMRR) at the operating frequency as reported by Boukabache et al [99] and Capineri et al [100].

4.2 Real time electronics for impact monitoring

In this section we review the developments on real time electronics for monitoring multiple impacts with multichannel inputs capability that is a mandatory feature for implementing large sensor network experiments and installation.

From the research point of view is also very important to test the whole SHM with multiple impacts to gather many signals in real time as shown by Ren et al [101]. This approach allows with laboratory experiments to simulate repetitive impacts at different energy levels and periods to test and optimize the sensor layout and electronic signal conditioning parameters. The multiple impact experiments can be done in laboratory with programmable mechanical impactors as reported in [39] and [22]. This solution is very useful for avoiding time consuming experiments based on pencil-lead break (PLB) tool for the collection of large signal data bases to test advanced algorithms (see Ebrahimkhanlou et al [96]). Impact detection and positioning is obtained with several sensors (at

least three) deployed on the structure with a strategy for uniform area coverage and detection sensitivity.

For these reasons, several recent works have proposed real-time electronic platform with multichannel capabilities to overcome the main limitation offered by the common solution of using a general-purpose digital oscilloscope. A real-time electronic platform design for passive and active mode functionalities was published by the authors Capineri et al [102], while Yuan et al [103] designed a low-cost signal acquisition system based on sensors tags with local preprocessing capability.

In early works published by Ziola [21], the evolution from narrow to broad bandwidth sensors and analog front-end systems was proposed to locate the acoustic source more accurately as the spatial resolution is improved by using higher frequency UGM. Impact velocity and energy variability generates different modes and for the calibration tests are often recommended low energy impacts carried out with the PLB as acoustic source, as reported by Wilcox et al [53]. The advantages of retrieving information from broadband signals are also discussed by Gao et al [104].

4.3 MEMS sensors, CMUT, PMUT and integration with electronics

The progresses of Micromachined Electrical Mechanical Systems (MEMS) in the last two decades have opened the research for a new class of sensors for AE and SHM. MEMS technology have received a great success to integrate sensors with electronics, especially for achieving mass production at low cost with integrated circuit technologies; tri-axial capacitive MEMS accelerometers is probably the first example of such integration process started in the 80's and now has achieved important results in multisensory nodes (MOTES) as reported by Glaser et al [105]. In

in this section the focus is about deterministic sensors for SHM and AE based on UGW both for passive and active mode as introduced in Section 2. The interest of deterministic sensor capable to directly produce flaw detection and flaw growth attracted the interest to find alternative to PZT, Aluminum Nitride (AlN), Zinc Oxide (ZnO) piezoelectric/piezoresistive UGW devices. Actuation and sensing UGWs by capacitive MEMS is derived by the first study of Haller et al [106] at Ginzton Laboratory, Stanford University, based on the electrostatic actuation of a thin silicon membrane. At first capacitive MEMS technology was meant for improving airborne ultrasonic transducers, but it revealed immediately the potential application for generating Lamb waves in solid materials (see Yaralioglu et al [107]); after two decades the recent advancement of capacitive MEMS sensors in design, fabrication and integration with electronics can be found in the review paper of B.T. Khury Yakub [108]. Since then, the effort for designing small scale factor Capacitive Micromachined Ultrasonic Transducers (CMUTs) for SHM and AE has been great and different design and fabrication methods have been proposed by PhD dissertation of Bradley [109] and recently by Butaud et al [110]. CMUTs are generally designed as resonant devices and the resonant frequency depends on the bias voltage. The front-end electronics for CMUT is generally different from that one required for low impedance piezoelectric devices; the essentially capacitive behavior of the sensor impedance requires a custom design of the LNA (see signal chain in Figure 10). In this regard for testing commercially available CMUTs in laboratory setups, charge amplifiers as CA7/C by Cooknell Electronics Ltd have been used by Bradley [109] and Butaud et al [110], while the opportunity to on chip integrated multichannel Analog Front-End (AFE) for CMUTs was reported by Savoia et al [111]; more recently the approach of monolithic integration of a CMUT array with

Application Specific Integrated Circuit (ASIC) based on flip-chip bonding has been presented by B.T. Khury-Yakub [108]. For the detection of Lamb waves, CMUTs need still to be improved in terms of sensitivity and signal to noise ratio respect to conventional piezoelectric sensors as reported by Boubenia et al [112]. MEMS technologies were also applied for designing and fabricating piezoelectric devices. Generally speaking, a piezoelectric MEMS sensor for SHM is based on a resonating silicon microstructure and a thin piezoelectric material layer and assembled in a ceramic package. The main advantage is to retain the high electromechanical coupling coefficient of piezoelectric materials with the advantage of a significant reduction in size and weight. The latter are promising features for an ease installation on structures and possible embedment. An alternative technology for sensor systems size reduction are Piezo-MEMS. There are two recent works published by Ozevin et al [113] reviewing the advancements of piezo-MEMS operating in the 40-200kHz frequency range. In the reference [114] are also reported MEMS based on both piezoresistive materials that need to be supplied by constant current sources and they need also to be temperature compensated; the same review work describes also another type of capacitive sensors for AE that differs from CMUT as it is based on the change of capacitance in response to a dynamic stimulus that varies the distance of the electrode plates. This principle well known in capacitive MEMS accelerometers is demonstrated for in plane wave sensing through a differential capacitance sensor for AE applications [115]. That review paper also addresses to the main difference between broadband and narrowband devices: while the latter have high sensitivity at the designed resonant frequency with high Q factor, the broadband are more versatile devices, but the sensitivity is not yet comparable with analog bulk piezoelectric sensors. The increase of active area of the piezo

MEMS increases the sensitivity but the footprint goes closer to those of conventional piezoelectric sensors. However, for some applications where high energy impacts generates large amplitude stress waves in the structure, the lower sensitivity of MEMS sensors can be acceptable. Despite these advantages of miniaturization and integration with AFE circuits, these devices lack of experimentation in harsh environment or at least in simulated operative conditions for aerospace, automotive and civil engineering applications. A recent review paper that discusses also the additional problems when the sensors are attached permanently to a structure has been published by Guemes et al [116]: the reliability of the entire SHM system needs to be studied with more focus in order to demonstrate the sensor and electronics technology for real life applications. Finally another MEMS technology investigated for AE sensor is the piezoelectric micromachined ultrasonic transducer (PMUT), first introduced in the 90's for ultrasonic applications in the 100kHz- 15 MHz range by Percin et al [117], Muralt et al [118] and Bernstein et al [119]. The main concept for the PMUT device was the design of a sensor based on laminated structures vibrating in the bending mode by combining rigidity and strain of beam and plate microstructures. This technology has been also applied recently for AE sensor and Feng et al [120] developed a PZT micromachined cantilever-based sensor. The comparison of the new PMUT device with a commercial sensor seems promising besides the characteristics (gain, bandwidth, filtering) of two adopted AFEs should be compared.

5. Hardware developments of wired and wireless sensor networks (WSNs) for SHM and validation tests.

From the previous sections it turns out that in the recent years the combination of several progresses in sensors and mixed signals low power electronics have introduced a new paradigm for the SHM

systems that is the network of sensors nodes, as reported by Farrar et al [121]. A conceptual description of the migration from single distributed sensors on a structure to the sensor network is shown in Figure 11, where for example the authors represented a sensor network for monitoring a COPV system. In the same picture are shown the main electronic blocks needed to realize a sensor node with active and passive mode operation. Both the transducer driver (for broadband or narrow band ultrasonic transducers) and the signal conditioning are controlled by a mixed signal System on Chip (SoC). The connections between nodes and the central unit (see architecture in Figure 9) can be implemented with wired solutions where the power lines for the nodes can sustain a sufficient data rate by using power line communication (PLC) protocols and related chipset. Simplified connection schemes and low power digital electronic front end has been recently proposed and validated on an aircraft wing by Qiu et al [72].

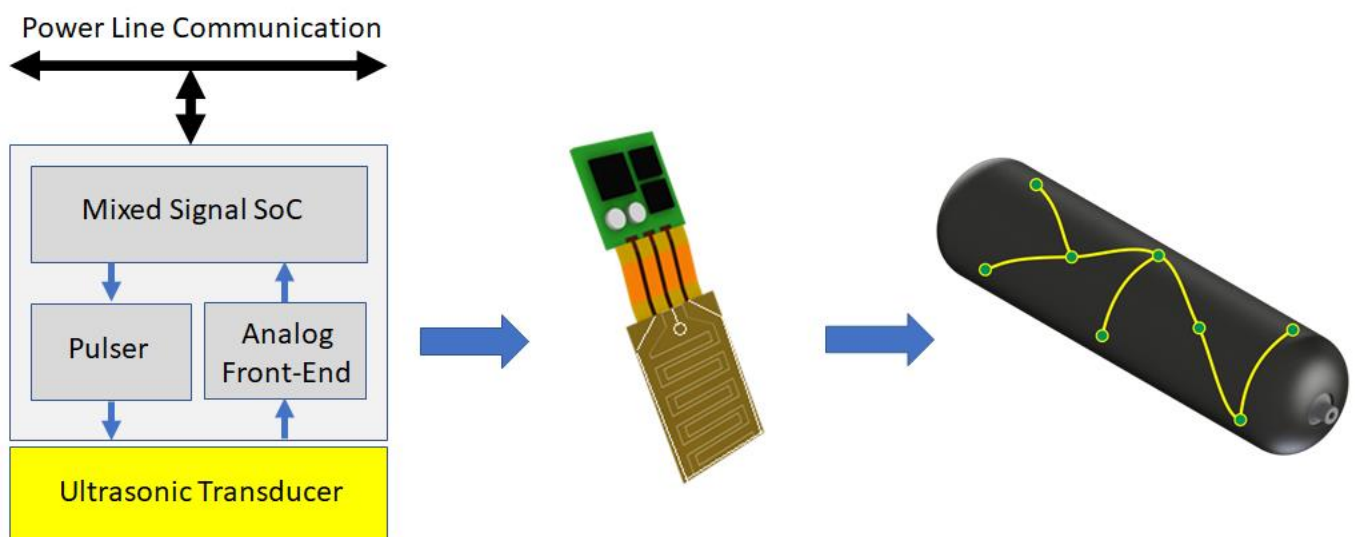


Figure 11 A wired sensor network based on autonomous sensor node design. In the example each node is equipped with an ultrasonic transducer for active and passive UGW operation: (a) node electronic block scheme; (b) node rendering; (c) rendering of a possible application to a COPV equipped with a wired sensor network.

One of the first implementation of this paradigm was published by Schubert et al [93] with the Match-X project of the Fraunhofer Institute. The node design and electronic integration with a stack

on miniaturized PCB with SMD components with embedded PZT transducers mounted on a glass-fiber-reinforced-polymer (GFRP) plate. The paper addressed also to the requirement of power supply overvoltage protection and detection of failure events that is one important consideration for self-diagnostic of nodes. Lehmann et al [42] presented in the same year the results of validation of the embedded PZT MFC transducers in an aircraft wing. Local processing of the acoustic signatures was demonstrated by the integration of the AFE in the node architecture: the ADC, and algorithms for data reduction, and digital communication thanks to the use of a Digital Signal Processor (DSP). Besides the adopted solution for data transfer was based on a two wires industrial Controller Area Network (CAN) bus, the authors introduced an expandable feature to open the wireless connection with a Bluetooth module, that recently have evolved in Wireless Sensor Networks (WSN). The main electronic blocks of a sensor node for a WSN are shown in Figure 12.

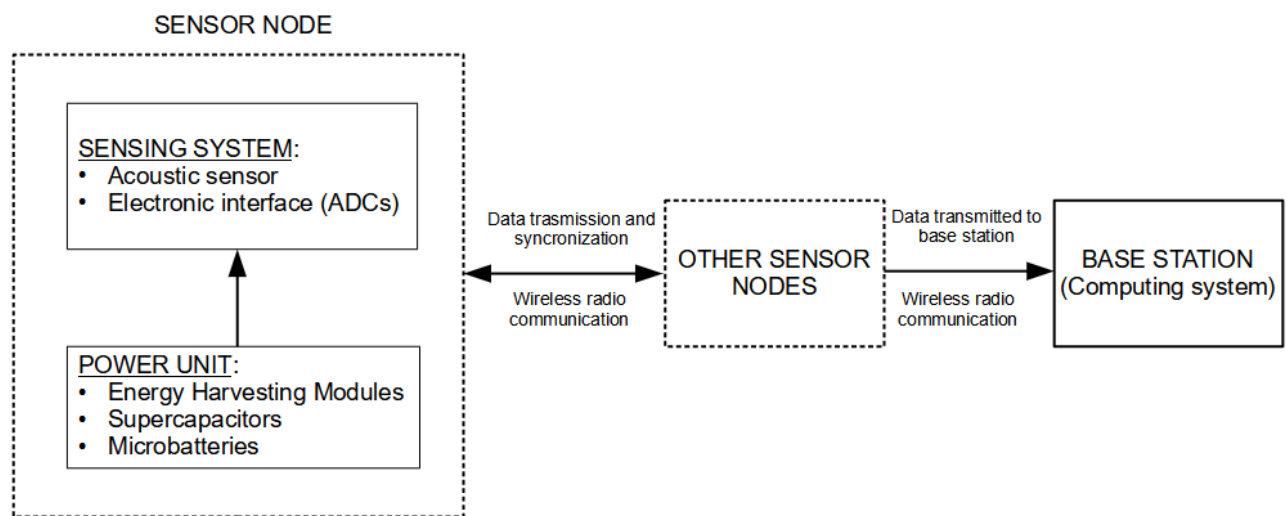


Figure 12 A block diagram of a wireless autonomous sensor network for SHM connected to a base station.

5.1 Nodes and modules with low power electronics solutions with energy harvesting

The main evolution for continuous impacts monitoring is the concept of autonomous nodes. In the case of an SHM system we can observe that environmental operating conditions as those described

in Figure 1, are represented by different type of energy exchanges with the structure. This interaction from the point of view of the impact event capture is seen as a disturbance or noise but from the point of view of local energy accumulation can represent an opportunity.

A preliminary work for this evolution was published by Champaigne et al [122] describing a SHM system with wireless connection to interface up to four PZT sensors but with the AFE capable to match different type of sensors. In that paper low power electronics available at that time was adopted to be compatible with charge capacity of a dual AA-cell battery pack to reach an operational time up to 10 total hours. A consideration must be made about the careful choice done for digital electronics such as the ADC, FPGA and digital communication, that are typically power angry devices. A recent paper that can solve the power demands for continuous monitoring is proposed by Fu et al [123] and the solutions consists of keeping in a sleep mode a section of the digital electronic processing until a detected event switches on the power supply of the data acquisition and processing blocks; a similar approach with a compact electronic design for a wireless smart sensor node was published by Overly et al [124]. In the latter work were used low power chips and self-diagnostic for the detection of PZT elements debonding from an aircraft wing. Another important design issue that is tackled in the paper, is the temporal synchronization of data from an impact event detected by the WSN; this topic will be expanded in the section 5.2. The design of a WSN with low power budget obtained by the sleep mode operability is presented by Giannì et al [125]; in particular the authors analyze the design issues regarding the AFE+ADC noise characteristics and their influence on the errors achievable for impact positioning with a triangulation method.

Ferin et al [94] presented a new hardware development of a highly versatile of energy autonomous acoustic sensor node that is an element of an intelligent wireless network, capable to host and run various ultrasonic inspection algorithms. The energy harvester was the conversion from mechanical vibrations into electrical energy stored in a supercapacitor with a high charge capacity/volume ratio. In this paper the hardware specifications for an automated and remote aircraft ultrasound inspection were considered as a start point for a product-oriented research. Taking advantage of low power electronics with energy harvesting solutions, the design of a MEMS piezoelectric power module converter with power density of $6\text{mW/cm}^3/\text{g}^2$ and an output power around $120\mu\text{W}$ was presented. To cover the full power supply demands of a sensor node, multiple MEMS power module can be connected at the expense of an increased volume occupation. The piezoelectric energy harvester system was capable to charge a thin film battery (EFL700A39 from STM - $700\mu\text{A/h}$ 3.9V). The topic of energy harvesting is strictly related to design autonomous sensor node and several review papers for the interested reader as Mateu et al [126], Sodano et al [127], Trigona et al [128] and an example of a small scale factor energy harvester device is reported in Figure 13. Authors presented in [128] a prototype system for delivering energy to SHM sensor nodes by microwave wireless energy transmission in the 10 GHz X-band. The energy harvesting for low power WSN with special emphasis to SMH application has been reviewed also by Park et al [129]. Finally, the outcomes of a recent project dedicated on the energy harvesting methods for SHM systems installed on airplanes have been published by Zelenika et al. [130].

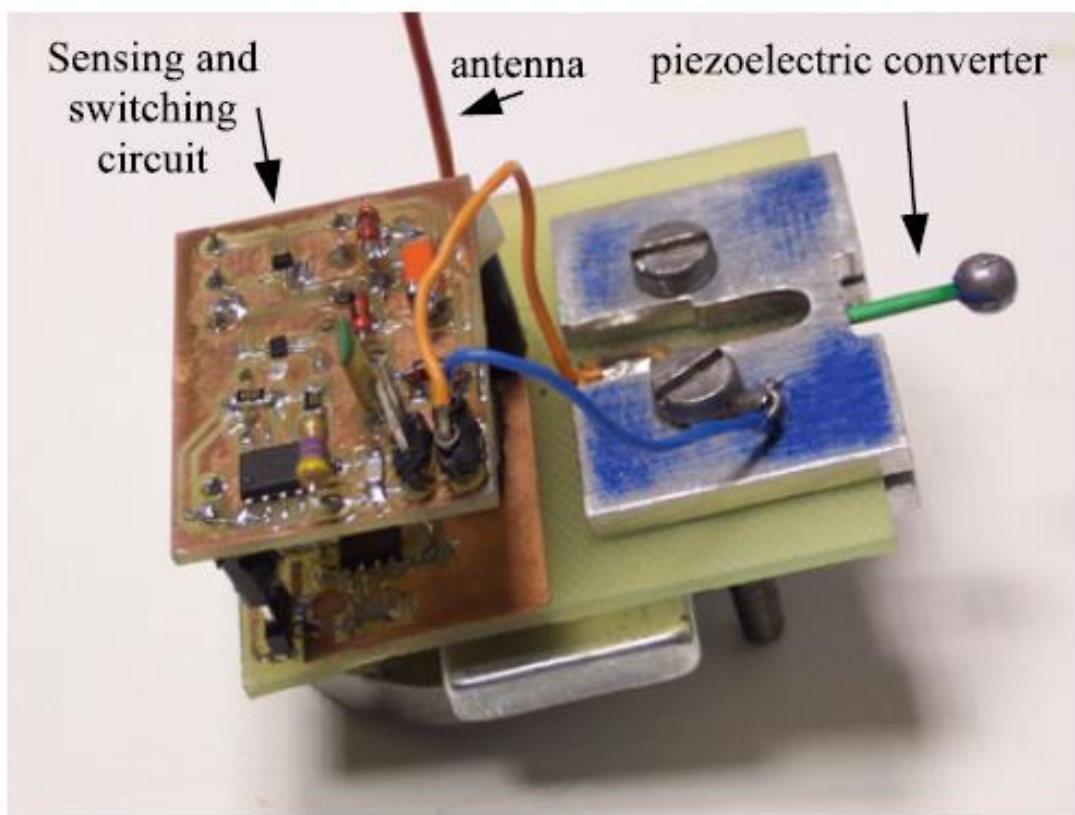
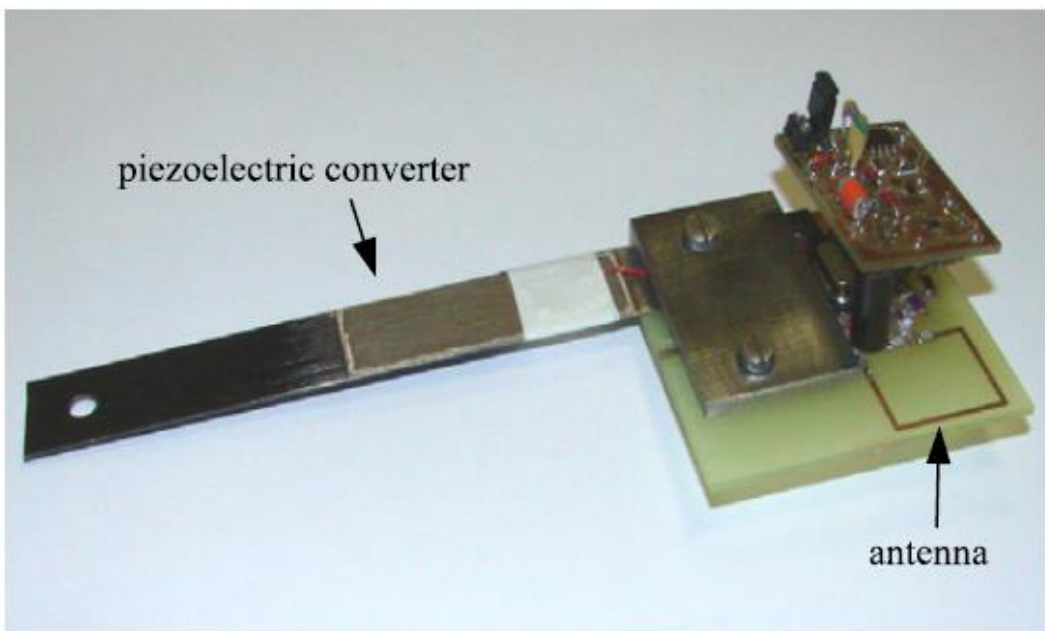


Figure 13 . The realized prototype of the autonomous sensor module with a thick-film piezoelectric converter (top) and with a commercial piezoelectric converter (bottom) (adapted from [131] with authors permission).

It is worth to mention also industrial projects covering the WSN approach for aircraft SHM as proposed by METIS Design company [132] and the European Project “FLite Instrumentation TEst Wireless Sensor”, [133]. Another kind of sensor network formed by modules connected by fiber optics to obtain large immunity from environmental electromagnetic noise, was presented by Smithard et al in [134]. The Acousto Ultrasonic Structural health monitoring Array Module (AUSAM) project relies on autonomous electronic modules designed with off-the shelf electronic components that interface up to 62 PWAS. These modules can operate in active and passive mode and are equipped also with an EMI module, the latter is usefully adopted for checking the reliability of the PWASs. A futuristic vision of the AUSAM module is the transportation and installation on the structure by a drone, with envisaged advantages on maintenance service performance and costs. A similar idea of using drones for EMI technique has been recently reported by Na et al [75]. The interest of sensor networks for SHM in transportation and civil engineering infrastructures also requires a different approach for system performance evaluation; Ju et al [135] proposed a simulation of a sensor network for continuous monitoring of railroads where fast transportation systems are in service. Sundaram et al [136] reviewed the advantages of WSN for SHM of large civil engineering structures and pointed out the problem of connection reliability, obstructions to radio links and finally the energy harvesting.

Ren et al [137] presented a strategy for radio communication of autonomous nodes for impact monitoring of large structure and a preliminary validation on a laboratory mock-up of an air wing is presented. The original solution is the adoption of a multi-channel radio communication on different frequency channels to improve the data transmission capability and the reliability of the WSN.

Embedded computational resources in sensors nodes for vibration monitoring has been designed and tested on a laboratory mock up by Testoni et al [138]; this work shows a design with volume/weigh constraints and power consumption of a node requirements for implementing a wired sensor network based with PCL.

Summarizing the outcomes of the works reviewed in this section we can say that are now available technologies for embedded signal processing, signal transmission with low power that can also be integrated with energy harvester devices that are mainly demonstrated in laboratory experiments, but some real-life cases started to be present in the literature. In the next section we will make a discussion of the issues for a wide spreading of smart nodes for SHM networks.

5.2 Toward SHM sensor networks with smart nodes

From the previous paragraph it is clear the interest to move SHM system toward sensor networks and in the following we draw some general comments and challenges for addressing the next steps for new developments. In this section we discuss the advancements of smart nodes in the perspective of an impact sensing SHM network.

One of the topics that is now under the attention of the research is the evaluation of data transfer requirements for a node. The reduction of data rate will bring the characteristic to change a node to a “smart-node” as some local processing is needed. The data rate reduction is achievable by compressive sensing techniques as investigated by Mascarenas in [139]. The recent research on this subject demonstrated also benefits for the autonomous detection and localization of an AE source, as we will explain later in section 6.

The presence of smart sensor nodes, and a relatively dense interconnection network, can provide some degree of redundancy to the SHM system, where failing sensor nodes will not compromise the operation of the overall system. Of course, the thickening of the interconnection network goes against the minimum-encumbrance policy, that is one of the original goals of the sensor network architecture, but it is a trade-off that should be considered, nonetheless. From the point of view of harnessing, PLC represent a way to achieve the minimum amount of cabling required to route the sensor network, albeit at the cost of reduced bandwidth. A problem that is deeply ingrained in sensor networks that need to cooperate in the ways described above is how to achieve and maintain inter-node synchronization. Although the topic has not been addressed so far, the problem of synchronization in measurement and control networks is well known and will be approached starting from the provisions of the Precise Time Protocol (PTP) IEEE 1588 standard that can reach a synchronization accuracy of $0.1 \mu\text{s}$ wired network connected on ethernet. Such performance is compatible with SHM sensor network design being the UGW signals with frequency content below 1MHz and Time of Flight (TOF) in the order of $10 \mu\text{s} - 100 \mu\text{s}$. This analysis derives from the main requirement that each sensor nodes need to be synchronized up to a fraction of the DToA to produce data useful for accurate impact positions. The synchronization problem is even more complex for WSNs and the next section will go in some detail of the proposed solutions.

5.3 WSN and IoT for SHM

In the last few years, the concept of WSN for SHM has moved on to the Internet of Things (IoT) for SHM. The main advantage of introducing the communication of a WSN for SHM over internet comes from the possibility to uniquely identify data packet generated a sensor node, large

bandwidth for data transmission and time correlation thanks to the accurate synchronization of nodes. Moreover, the large storage capacity of the cloud allows to implement further the data interpretation by using AI and deep learning for Big Data (BD); some examples of the latter novel development will be reported in the next section.

Tokognon et al [140] have well reviewed the challenges for the design SHM using IoT technologies to achieve intelligent and reliable WSN for monitoring structures. The authors identify three main blocks to be integrated for this aim:

- Sensing and data Acquisition Subsystem.
- Data Management Subsystem: preprocessing methods used to organize raw data acquired from sensors and remove noise before processing; novelty detection, classification, and regression approaches. Among them, novelty detection based on artificial neural networks.
- Data Access and Retrieval Subsystem.

The requirement of low power communication technology based on IPv6 assignment of a node is analyzed for battery operated sensors. ZigBee Alliance working has accelerated the expansion of the sensor network and building automation market. From the PHY and MAC layers defined in the IEEE 802.15.4 standards Zigbee considers networking and services layer, through the full application layer. ZigBee PRO was developed specifically for device-to-device communication in IoT context.

Unfortunately, WSN based on IEEE 802.15.4/ZigBee do not currently support IP, mainly due to the small length of packets used in IEEE 802.15.4. Therefore, most of the solutions proposed consist of using IP proxy or gateways. A network configuration strategy for WSN configuration with sink nodes at the edge of the network, also called border routers, with IP protocol connection over Internet is presented in the paper by Tokognon et al [140]. From the sink nodes data can be transferred with JavaScript object notation (JSON) to a Web server where a large storage capacity is commonly available.

Moreover, the Internet Engineering Task Force (IETF) defined the 6LoWPAN standard (RFC 4944) to allow the use of IPv6 packets over IEEE802.15.4 networks. It compressed IP headers to resolve packets size issue and fragmentation mechanism to transmit IP packets over IEEE802.15.4 networks. IETF also started a working group to evaluate appropriate routing protocols for low-power (RPL) and lossy networks.

As stated in the previous section the node synchronization is another challenge for a distributed IoT. Scuro et al [141] published a work devoted to this problem and a solution was proposed with each is equipped with a clock, and typically they exchange synchronization messages to evaluate the frequency and the offset of their clock with respect to one taken as reference (master) or with respect to its neighbor sensor node. This solution implies an additional overhead, since extra messages and re-synchronization periods are required.

In the same structure, local area networks with routers that give priority to the transmission of the synchronization messages, or that compensate for the transmission delay, can be deployed. In these cases, synchronization accuracy in the order of microseconds is still achievable. In fact, for the SHM

system the typical accuracy needed between the node is in the range $[0.6, 9.0]\mu\text{s}$. Muttillo et al [142] presented a solution for structural monitoring with digital accelerometers ADXL355 with high resolution connected to hardware for IoT connection. To preserve such performance a high synchronization between the sensors was implemented.

Finally, example of prototype architectures for WSN nodes connected on ethernet based on Raspberry Pi have been presented by Abdelgawad et al [143] and Mahmud et al [144]. Besides the power consumption of these design was a neglected factor, the two systems were successfully demonstrated for SHM in laboratory.

6. Artificial Intelligence and Machine Learning.

The previous sections pointed out how embedded sensors with low power electronics in a sensor node enable SHM monitoring networks on IoT for large and complex structures. This new paradigm also brings the large data collection and data interpretation challenges. In this section are discussed the recent approaches based on BD and Artificial Intelligence (AI) and then we complete the review of all SHM system components shown in Figure 1.

One of the early papers on this subject was published by Farrar and Worden [5]. The authors pioneered this subject with the introduction of the machine learning/statistical pattern recognition paradigm for SHM. Since then, in the last decades remarkable developments have been done.

Worden et al [145] analyzed the non-stationary properties of the Lamb waves used in SHM and how the machine learning approach can solve the operator-based data interpretation that results difficult and time consuming.

As said above, BD can potentially enable the automatic classification of defects, but the reduction of input data remains a goal to simplify the design of the processing task, as proposed by Bao et al [146]. The application of compressive sampling of sensors signals is a useful strategy and in particular for Lamb waves, it is worth to mention the work of Bao et al [146] where a CNN was trained with experimental data.

Yuhan et al [147] observed that in many practical situations the data set are limited to a small period of monitoring time and generated by a specific part of a complex structure and this limits the performance achievable with ML. That work analyzed a possible solution based on physics-informed learning, that integrate information derived from physics-based model into the learning process. Examples of physics-informed Deep Learning (DL) approach applied for low-velocity impact diagnosis is reported. For this aim a pipeline consisting of a unified CNN-RNN network architecture for spatial-temporal analysis of the impact generated wavefield was developed. The knowledge type of physical principles was based on classic Huygens principle, time-reversal methods Fink et al [33] and simulated data based on dispersive propagation model of generated waves from impacts. This knowledge was introduced in the CNN network of the data processing pipeline and helps to define a vector feature for the learning and classification. The autonomous detection of defects in plate-like metal panels was investigated by Hesser et al [148] with a ANN trained by signals acquired by four commercial sensors (PIC255 from PI Ceramic) with 1 MHz sampling rate and 16 bit resolution ADC. The experimental data set was generated by free falling ball impact at low velocity (about 1 m/s) that are converted in large amplitude, low phase velocity A_0 mode Lamb waves. By this approach is demonstrated that the achievable spatial accuracy is in

the order of the wavelength corresponding to the main A_0 received mode with frequency content well below 100 kHz. Another paper following the work of Hesser is published by Mariani et al [149] where the autonomous defects classification is explored with a CNN approach that overcome the limitations of extensive baseline data archives.

Sun et al [150] have reviewed the framework for the development of damage detection in civil engineering infrastructures (bridges) where big data can be acquired in real time and artificial intelligence strategies need to be adopted.

An interesting approach based on data driven models, is the application of DL with ANN to directly input raw data from a limited number of sensors for impact localization and characterization is published by Ebrahimkhanlou et al [96]. In that paper a deep network is trained on simulated and experimental data sets with signals received by a very small number of sensors (from 1 to 4) covering the area of a test aluminum panel equal to 500mm x 500 mm. The single sensor solution is certainly attractive from the point of view of cabling and costs but for the system reliability a certain degree of redundancy is necessary by increasing the number of sensors which also improves the accuracy of impact area estimate and impact characterization.

Another example in the literature is from Melville et al. [151]; the authors reported the investigation of Lamb waves generated in an aluminum laminate by piezoelectric transducers, although they used a SLDV to acquire images of the full wavefield, then used a Convolutanional Neural Network (CNN) for the interpretation. Finally, we observe that the DL approach is capable to exploit

information from signals acquired over a long-time interval, where multimodal dispersion and reverberations (multipath) effects are present.

7. Conclusions

The paper examines recent developments in integrated SHM sensors and systems for impact detection. The design of advanced SHM systems for impact monitoring benefits from recent advances in UGW modeling, sensor materials for MEMS solutions and interface electronics, signal processing algorithms for real-time applications, sensors for WSN and IOT and data processing with AI and Big Data.

In the first part of the work the characteristics of the UGW modes generated by the impacts are discussed with the differentiation of low and high speed impacts and their attenuation. The main concepts of this physical background are reported because they are relevant to indicate the different characteristics (amplitude, spectral content, modes velocity dispersion) of the signals that must be processed by the front-end electronics. Then the characteristics of the most common wideband patch type piezoelectric sensors (PWAS) with narrowband IDT used for Lamb wave mode selection, are compared. The introduction of new piezoelectric materials (Carbon Nano Tubes, Microfiber Composites) for MEMS sensors for detecting impact signals is more recent but promising results have been reported; CMUT and PMUT devices have also a good perspective to be used in SHM for their inherent advantage of the electronics integration. The paper also addresses the design issues for front-end electronics that must match sensor characteristics and impact signals with different energy and operating in the bandwidth 50 kHz-1MHz. A particular attention to on-site

environmental factors (e.g. thermal excursion, deformation, vibrations) were also discussed because they influence the choice of the sensor technology; for the compensation of environmental factors, the research trend is the design of multifunctional sensor nodes and ad-hoc algorithms. The document also shows examples of real SHM installations with operability in passive mode and active mode for damage assessment.

A new emerging technology to reduce the complexity of wired sensor networks is the adoption of a "smart skin" with stretchable / flexible piezoelectric sensors. The analysis of several papers on this topic, indicates that a trade-off can be achieved between the number of sensors installed and the coverage of the entire area under test. The first part of the review concludes with the description of recent developments on integrated or embedded electronic systems with hardware system on chip with small footprint design.

In the second part of the review, are reported the advances in sensor technology with low-power mixed-signal electronics that have changed the architectural design of SHM systems by introducing the concept of "autonomous intelligent nodes". This type of devices have a microprocessor on board, different types of sensors, wireless communication, locally powered and are low cost. Autonomous sensor nodes will also use MEMS devices for energy harvesting in the future, with power conversion capability above $100\mu\text{W}$ and high power density. Wireless communication of a node is now more common as reliable communication over different frequency channels has been demonstrated. The main reasons for the introduction of the WSN for SHM on the Internet derive from the ability to identify the data packets transmitted by a node and the exploitation of synchronization techniques with latency better than $1\ \mu\text{s}$ to correlate the sampled signals generated

by an event of impact. The latency in communication between WSN nodes affects the differential time of arrival error, which is one of the key information for impact positioning. We can summarize that in the future it will be increasingly common to monitor large facilities with sensor networks on the IoT due to the integration of sensors, low-power analog and digital electronics and efficient wireless communication.

For the off-site components of the SHM system, the document introduces in the last section the new challenge of interpreting the impact event on complex structures by collecting large data. Since the complexity of the problem is high, several promising works based on Big Data (BD) and Artificial Intelligence (AI) show that the localization of an impact is obtainable with errors comparable to deterministic algorithms applicable only for simple structures.

Overall, the authors of this paper have set themselves the goal of providing a useful reference for readers interested in the design, use and development of on-site and off-site components of advanced ultrasonic wave guided SHM systems.

References

1. Rose, J.L. *Ultrasonic Guided Waves in Solid Media*; Cambridge University Press: New York, 2014; ISBN 978-1-107-27361-0.
2. Auld, B.A. *Acoustic Fields and Waves in Solids*; Wiley: New York, 1973; ISBN 978-0-471-03702-6.
3. Farrar, C.R.; Worden, K. An Introduction to Structural Health Monitoring. *Philos. Trans. R. Soc. Math. Phys. Eng. Sci.* **2007**, 365, 303–315, doi:10.1098/rsta.2006.1928.
4. Farrar, C.R.; Worden, K. An Introduction to Structural Health Monitoring. In *New Trends in Vibration Based Structural Health Monitoring*; Deraemaeker, A., Worden, K., Eds.; CISM International Centre for Mechanical Sciences; Springer Vienna: Vienna, 2010; Vol. 520, pp. 1–17 ISBN 978-3-7091-0398-2.

5. Farrar, C.R.; Worden, K. *Structural Health Monitoring: A Machine Learning Perspective*; John Wiley & Sons, Ltd: Chichester, UK, 2012; ISBN 978-1-118-44311-8.
6. Mitra, M.; Gopalakrishnan, S. Guided Wave Based Structural Health Monitoring: A Review. *Smart Mater. Struct.* **2016**, *25*, 053001, doi:10.1088/0964-1726/25/5/053001.
7. Giurgiutiu, V. *Structural Health Monitoring with Piezoelectric Wafer Active Sensors*; Academic Press, an imprint of Elsevier: Amsterdam, 2014; ISBN 978-0-12-418691-0.
8. Zhou, G.; Sim, L.M. Damage Detection and Assessment in Fibre-Reinforced Composite Structures with Embedded Fibre Optic Sensors-Review. *Smart Mater. Struct.* **2002**, *11*, 925–939, doi:10.1088/0964-1726/11/6/314.
9. Kirkby, E.; de Oliveira, R.; Michaud, V.; Månsen, J.A. Impact Localisation with FBG for a Self-Healing Carbon Fibre Composite Structure. *Compos. Struct.* **2011**, *94*, 8–14, doi:10.1016/j.compstruct.2011.07.030.
10. Shin, C.S.; Chen, B.L. An Impact Source Locating System Using Fiber Bragg Grating Rosette Array.; Shenzhen, China, April 2 2012; p. 84091B.
11. Yeager, M.; Whittaker, A.; Todd, M.; Kim, H.; Key, C.; Gregory, W. Impact Detection and Characterization in Composite Laminates with Embedded Fiber Bragg Gratings. *Procedia Eng.* **2017**, *188*, 156–162, doi:10.1016/j.proeng.2017.04.469.
12. Datta, A.; Augustin, M.J.; Gupta, N.; Viswamurthy, S.R.; Gaddikeri, K.M.; Sundaram, R. Impact Localization and Severity Estimation on Composite Structure Using Fiber Bragg Grating Sensors by Least Square Support Vector Regression. *IEEE Sens. J.* **2019**, *19*, 4463–4470, doi:10.1109/JSEN.2019.2901453.
13. Roach, D.P. FAA Research Program Webinar Series on Structural Health Monitoring - Module 1: Introduction to SHM and Implementation. **2016**.
14. Shen, G.; Zhang, J.; Lackner, G. International Acoustic Emission Standard Analysis and Development Outlook. *Insight - Non-Destr. Test. Cond. Monit.* **2020**, *62*, 724–734, doi:10.1784/insi.2020.62.12.724.
15. Ono, K. Review on Structural Health Evaluation with Acoustic Emission. *Appl. Sci.* **2018**, *8*, 958, doi:10.3390/app8060958.
16. Rose, J. Ultrasonic Guided Waves in Structural Health Monitoring. *Key Eng. Mater. - KEY ENG MAT* **2004**, 270–273, 14–21, doi:10.4028/www.scientific.net/KEM.270-273.14.
17. Mallardo, V.; Aliabadi, M.H. Optimal Sensor Placement for Structural, Damage and Impact Identification: A Review. *SDHM Struct. Durab. Health Monit.* **2013**, *9*, doi:10.32604/sdhm.2013.009.287.
18. Safri, S.; Sultan, M.T.H.; Yidris, N.; Mustapha, F. Low Velocity and High Velocity Impact Test on Composite Materials - A Review. *Int. J. Eng. Sci.* **2014**, *3*, 50–60.
19. Ross, R. Structural Health Monitoring and Impact Detection Using Neural Networks for Damage Characterization.; 2006; Vol. 9.
20. Tobias, A. Acoustic-Emission Source Location in Two Dimensions by an Array of Three Sensors. *Non-Destr. Test.* **1976**, *9*, 9–12, doi:10.1016/0029-1021(76)90027-X.
21. Ziola, S.M.; Gorman, M.R. Source Location in Thin Plates Using Cross-correlation. *J. Acoust. Soc. Am.* **1991**, *90*, 2551–2556, doi:10.1121/1.402348.
22. Marino-Merlo, E.; Bulletti, A.; Giannelli, P.; Calzolai, M.; Capineri, L. Analysis of Errors in the Estimation of Impact Positions in Plate-Like Structure through the Triangulation Formula by Piezoelectric Sensors Monitoring. *Sensors* **2018**, *18*, 3426, doi:10.3390/s18103426.
23. Gorman, M.R.; Humes, D.H.; June, R.; Prosser, W.H.; Prosser, W.H. Acoustic Emission Signals in Thin Plates Produced by Impact Damage. *J. Acoust. Emiss.* **1999**, *17*, 29–36.
24. Yang, J.C.S.; Chun, D.S.; MD, N.O.L.W.O. *Application of the Hertz Contact Law to Problems of Impact in Plates*; Defense Technical Information Center, 1969;

25. Richardson, M. Measurement and Analysis of the Dynamics of Mechanical Structures. *J. Acoust. Soc. Am.* **1979**, *65*, S77–S77, doi:10.1121/1.2017435.

26. Staszewski, W.J.; Mahzan, S.; Traynor, R. Health Monitoring of Aerospace Composite Structures – Active and Passive Approach. *Compos. Sci. Technol.* **2009**, *69*, 1678–1685, doi:10.1016/j.compscitech.2008.09.034.

27. On Waves in an Elastic Plate. *Proc. R. Soc. Lond. Ser. Contain. Pap. Math. Phys. Character* **1917**, *93*, 114–128, doi:10.1098/rspa.1917.0008.

28. Bulletti, A.; Merlo, E.M.; Capineri, L. Analysis of the Accuracy in Impact Localization Using Piezoelectric Sensors for Structural Health Monitoring with Multichannel Real-Time Electronics. In Proceedings of the 2020 IEEE 7th International Workshop on Metrology for AeroSpace (MetroAeroSpace); IEEE: Pisa, Italy, June 2020; pp. 480–484.

29. Chandrasekaran, S. *Structural Health Monitoring with Application to Offshore Structures*; WORLD SCIENTIFIC, 2019; ISBN 9789811201080.

30. Miniaci, M.; Mazzotti, M.; Radzieński, M.; Kudela, P.; Kherraz, N.; Bosia, F.; Pugno, N.M.; Ostachowicz, W. Application of a Laser-Based Time Reversal Algorithm for Impact Localization in a Stiffened Aluminum Plate. *Front. Mater.* **2019**, *6*, 30, doi:10.3389/fmats.2019.00030.

31. Nicassio, F.; Carrino, S.; Scarselli, G. Non-Linear Lamb Waves for Locating Defects in Single-Lap Joints. *Front. Built Environ.* **2020**, *6*, 45, doi:10.3389/fbuil.2020.00045.

32. Mevissen, F.; Meo, M. A Nonlinear Ultrasonic Modulation Method for Crack Detection in Turbine Blades. *Aerospace* **2020**, *7*, 72, doi:10.3390/aerospace7060072.

33. Fink, M. Time Reversal Mirrors. In *Acoustical Imaging*; Jones, J.P., Ed.; Acoustical Imaging; Springer US: Boston, MA, 1995; Vol. 21, pp. 1–15 ISBN 978-1-4613-5797-1.

34. Mariani, S.; Liu, Y.; Cawley, P. Improving Sensitivity and Coverage of Structural Health Monitoring Using Bulk Ultrasonic Waves. *Struct. Health Monit.* **2020**, *147592172096512*, doi:10.1177/1475921720965121.

35. Mariani, S.; Heinlein, S.; Cawley, P. Location Specific Temperature Compensation of Guided Wave Signals in Structural Health Monitoring. *IEEE Trans. Ultrason. Ferroelectr. Freq. Control* **2020**, *67*, 146–157, doi:10.1109/TUFFC.2019.2940451.

36. Sepehry, N.; Shamshirsaz, M.; Abdollahi, F. Temperature Variation Effect Compensation in Impedance-Based Structural Health Monitoring Using Neural Networks. *J. Intell. Mater. Syst. Struct.* **2011**, *22*, 1975–1982, doi:10.1177/1045389X11421814.

37. Qing, X.; Li, W.; Wang, Y.; Sun, H. Piezoelectric Transducer-Based Structural Health Monitoring for Aircraft Applications. *Sensors* **2019**, *19*, 545, doi:10.3390/s19030545.

38. De Simone, M.E.; Ciampa, F.; Boccardi, S.; Meo, M. Impact Source Localisation in Aerospace Composite Structures. *Smart Mater. Struct.* **2017**, *26*, 125026, doi:10.1088/1361-665X/aa973e.

39. Seno; Aliabadi Impact Localisation in Composite Plates of Different Stiffness Impactors under Simulated Environmental and Operational Conditions. *Sensors* **2019**, *19*, 3659, doi:10.3390/s19173659.

40. Kundu, T.; Das, S.; Jata, K.V. Point of Impact Prediction in Isotropic and Anisotropic Plates from the Acoustic Emission Data. *J. Acoust. Soc. Am.* **2007**, *122*, 2057–2066, doi:10.1121/1.2775322.

41. Hakoda, C.; Lissenden, C. Using the Partial Wave Method for Wave Structure Calculation and the Conceptual Interpretation of Elastodynamic Guided Waves. *Appl. Sci.* **2018**, *8*, 966, doi:10.3390/app8060966.

42. Lehmann, M.; Büter, A.; Frankenstein, B.; Schubert, F.; Brunner, B. *Monitoring System for Delamination Detection - Qualification of Structural Health Monitoring (SHM) Systems*; 2006;

43. Scheerer, M.; Lager, D. *DEVELOPMENT AND TESTING OF A HYBRIDE ACTIVE – PASSIVE ACOUSTIC SHM SYSTEM FOR IMPACT DAMAGE DETECTION IN HONEYCOMB AIRCRAFT STRUCTURES*; 2013;

44. Ebrahimkhanlou, A.; Salamone, S. Acoustic Emission Source Localization in Thin Metallic Plates: A Single-Sensor Approach Based on Multimodal Edge Reflections. *Ultrasonics* **2017**, *78*, 134–145, doi:10.1016/j.ultras.2017.03.006.

45. Park, W.H.; Packo, P.; Kundu, T. Acoustic Source Localization in an Anisotropic Plate without Knowing Its Material Properties – A New Approach. *Ultrasonics* **2017**, *79*, 9–17, doi:10.1016/j.ultras.2017.02.021.

46. Ren, B.; Lissenden, C.J. PVDF Multielement Lamb Wave Sensor for Structural Health Monitoring. *IEEE Trans. Ultrason. Ferroelectr. Freq. Control* **2016**, *63*, 178–185, doi:10.1109/TUFFC.2015.2496423.

47. Altammar, H.; Dhingra, A.; Salowitz, N. Ultrasonic Sensing and Actuation in Laminate Structures Using Bondline-Embedded D35 Piezoelectric Sensors. *Sensors* **2018**, *18*, 3885, doi:10.3390/s18113885.

48. Ciampa, F.; Meo, M. A New Algorithm for Acoustic Emission Localization and Flexural Group Velocity Determination in Anisotropic Structures. *Compos. Part Appl. Sci. Manuf.* **2010**, *41*, 1777–1786, doi:10.1016/j.compositesa.2010.08.013.

49. Kundu, T. Acoustic Source Localization. *Ultrasonics* **2014**, *54*, 25–38, doi:10.1016/j.ultras.2013.06.009.

50. Marchi, L.D.; Marzani, A.; Speciale, N.; Viola, E. A Passive Monitoring Technique Based on Dispersion Compensation to Locate Impacts in Plate-like Structures. *Smart Mater. Struct.* **2011**, *20*, 035021, doi:10.1088/0964-1726/20/3/035021.

51. Si, L.; Baier, H. Real-Time Impact Visualization Inspection of Aerospace Composite Structures with Distributed Sensors. *Sensors* **2015**, *15*, 16536–16556, doi:10.3390/s150716536.

52. Zeng, L.; Lin, J.; Huang, L. A Modified Lamb Wave Time-Reversal Method for Health Monitoring of Composite Structures. *Sensors* **2017**, *17*, 955, doi:10.3390/s17050955.

53. Scholey, J.; Wilcox, P.; Wisnom, M.; Friswell, M.; Pavier, M.J.; Aliha, M.R.M. A Generic Technique for Acoustic Emission Source Location. *J Acoust. Emis* **2009**, *27*.

54. Morón, C.; Portilla, M.; Somolinos, J.; Morales, R. Low-Cost Impact Detection and Location for Automated Inspections of 3D Metallic Based Structures. *Sensors* **2015**, *15*, 12651–12667, doi:10.3390/s150612651.

55. Nucera, C.; White, S.; Chen, Z.M.; Kim, H.; Lanza di Scalea, F. Impact Monitoring in Stiffened Composite Aerospace Panels by Wave Propagation. *Struct. Health Monit. Int. J.* **2015**, *14*, 547–557, doi:10.1177/1475921715599600.

56. Giurgiutiu, V. *Structural Health Monitoring with Piezoelectric Wafer Active Sensors*; Academic Press, an imprint of Elsevier: Amsterdam, 2014; ISBN 978-0-12-418691-0.

57. Monkhouse, R.S.C.; Wilcox, P.W.; Lowe, M.J.S.; Dalton, R.P.; Cawley, P. The Rapid Monitoring of Structures Using Interdigital Lamb Wave Transducers. *Smart Mater. Struct.* **2000**, *9*, 304–309, doi:10.1088/0964-1726/9/3/309.

58. Mujica, L.; Rodellar, J.; Vehí, J. A Review of Impact Damage Detection in Structures Using Strain Data. *Int. J. COMADEM* **2010**, *13*, 3–18.

59. IZFP, C.C.; Wu, K.; Sun, Z.; Mrad, N. A COMPARATIVE STUDY ON TWO FAMILIES OF INTEGRATABLE ULTRASOUND TRANSDUCERS FOR STRUCTURAL HEALTH MONITORING.; 2011.

60. Bulletti, A.; Giannelli, P.; Calzolai, M.; Capineri, L. An Integrated Acousto/Ultrasonic Structural Health Monitoring System for Composite Pressure Vessels. *IEEE Trans. Ultrason. Ferroelectr. Freq. Control* **2016**, *63*, 864–873, doi:10.1109/TUFFC.2016.2545716.

61. Stepinski, T.; Mańka, M.; Martowicz, A. Interdigital Lamb Wave Transducers for Applications in Structural Health Monitoring. *NDT E Int.* **2017**, *86*, 199–210, doi:10.1016/j.ndteint.2016.10.007.

62. Gardiner, G. [Https://Www.Compositesworld.Com/Articles/Structural-Health-Monitoring-Ndt-Integrated-Aerostructures-Enter-Service](https://Www.Compositesworld.Com/Articles/Structural-Health-Monitoring-Ndt-Integrated-Aerostructures-Enter-Service).

63. Qi, B.; Kong, Q.; Qian, H.; Patil, D.; Lim, I.; Li, M.; Liu, D.; Song, G. Study of Impact Damage in PVA-ECC Beam under Low-Velocity Impact Loading Using Piezoceramic Transducers and PVDF Thin-Film Transducers. *Sensors* **2018**, *18*, 671, doi:10.3390/s18020671.

64. Jia, Y.; Chen, X.; Ni, Q.; Li, L.; Ju, C. Dependence of the Impact Response of Polyvinylidene Fluoride Sensors on Their Supporting Materials' Elasticity. *Sensors* **2013**, *13*, 8669–8678, doi:10.3390/s130708669.

65. Han, J.; Li, D.; Zhao, C.; Wang, X.; Li, J.; Wu, X. Highly Sensitive Impact Sensor Based on PVDF-TrFE/Nano-ZnO Composite Thin Film. *Sensors* **2019**, *19*, 830, doi:10.3390/s19040830.

66. Capsal, J.-F.; David, C.; Dantras, E.; Lacabanne, C. Piezoelectric Sensing Coating for Real Time Impact Detection and Location on Aircraft Structures. *Smart Mater. Struct.* **2012**, *21*, 055021, doi:10.1088/0964-1726/21/5/055021.

67. Kwon, H.; Park, Y.; Shin, C.; Kim, J.-H.; Kim, C.-G. Embedded Silicon Carbide Fiber Sensor Network Based Low-Velocity Impact Localization of Composite Structures. *Smart Mater. Struct.* **2020**, *29*, 055030, doi:10.1088/1361-665X/ab7946.

68. Aly, K.; Bradford, P.D. Real-Time Impact Damage Sensing and Localization in Composites through Embedded Aligned Carbon Nanotube Sheets. *Compos. Part B Eng.* **2019**, *162*, 522–531, doi:10.1016/j.compositesb.2018.12.104.

69. Bellan, F.; Bulletti, A.; Capineri, L.; Masotti, L.; Yaralioglu, G.G.; Degertekin, F.L.; Khuri-Yakub, B.T.; Guasti, F.; Rosi, E. A New Design and Manufacturing Process for Embedded Lamb Waves Interdigital Transducers Based on Piezopolymer Film. *Sens. Actuators Phys.* **2005**, *123–124*, 379–387, doi:10.1016/j.sna.2005.05.013.

70. Ghoshal, A.; Prosser, W.H.; Kim, H.S.; Chattopadhyay, A.; Copeland, B. Development of Embedded Piezoelectric Acoustic Sensor Array Architecture. *Microelectron. Reliab.* **2010**, *50*, 857–863, doi:10.1016/j.microrel.2010.01.037.

71. Adreades, C.; Ciampa, F. Embedded Piezoelectric Transducers in Carbon Fibre Composites for Nonlinear Ultrasonic Applications. In Proceedings of the Structural Health Monitoring 2017; DEStech Publications, Inc., September 28 2017.

72. Qiu, L.; Deng, X.; Yuan, S.; Huang, Y.; Ren, Y. Impact Monitoring for Aircraft Smart Composite Skins Based on a Lightweight Sensor Network and Characteristic Digital Sequences. *Sensors* **2018**, *18*, 2218, doi:10.3390/s18072218.

73. Kurita, H.; Wang, Z.; Nagaoka, H.; Narita, F. Fabrication and Mechanical Properties of Carbon-Fiber-Reinforced Polymer Composites with Lead-Free Piezoelectric Nanoparticles. *Sens. Mater.* **2020**, *32*, 2453, doi:10.18494/SAM.2020.2820.

74. Kopsaftopoulos, F.; Chang, F.-K. A Dynamic Data-Driven Stochastic State-Awareness Framework for the Next Generation of Bio-inspired Fly-by-Feel Aerospace Vehicles. In *Handbook of Dynamic Data Driven Applications Systems*; Blasch, E., Ravela, S., Aved, A., Eds.; Springer International Publishing: Cham, 2018; pp. 697–721 ISBN 978-3-319-95503-2.

75. Na, W.; Baek, J. A Review of the Piezoelectric Electromechanical Impedance Based Structural Health Monitoring Technique for Engineering Structures. *Sensors* **2018**, *18*, 1307, doi:10.3390/s18051307.

76. Hu, H.; Zhu, X.; Wang, C.; Zhang, L.; Li, X.; Lee, S.; Huang, Z.; Chen, R.; Chen, Z.; Wang, C.; et al. Stretchable Ultrasonic Transducer Arrays for Three-Dimensional Imaging on Complex Surfaces. *Sci. Adv.* **2018**, *4*, eaar3979, doi:10.1126/sciadv.aar3979.

77. Martowicz, A.; Rosiek, M.; Manka, M.; Uhl, T. Design Process of IDT Aided by Multiphysics FE Analyses. *Int. J. Multiphysics* **2012**, *6*, 129–148, doi:10.1260/1750-9548.6.2.129.

78. Lugovtsova, Y.; Bulletti, A.; Giannelli, P.; Capineri, L.; Prager, J. Characterization of a Flexible Piezopolymer-Based Interdigital Transducer for Selective Excitation of Ultrasonic Guided Waves. In Proceedings of the 2020 IEEE International Ultrasonics Symposium (IUS); IEEE: Las Vegas, NV, USA, September 7 2020; pp. 1–4.

79. Bulletti, A.; Giannelli, P.; Calzolai, M.; Capineri, L. Multielement Interdigital Transducers for Structural Health Monitoring. In Proceedings of the 2018 IEEE International Ultrasonics Symposium (IUS); IEEE: Kobe, October 2018; pp. 1–3.

80. Thompson, D.O.; Chimenti, D.E. Review of Progress in Quantitative Nondestructive Evaluation: Volume 17A.

81. Wang, Z.; Tang, T.; Chen, S.; Chen, B. Field Analysis and Calculation of Interdigital Transducers with Arbitrary Finger Shapes. *J. Phys. Appl. Phys.* **2006**, *39*, 4902–4908, doi:10.1088/0022-3727/39/22/024.

82. Mańka, M.; Rosiek, M.; Martowicz, A.; Stepinski, T.; Uhl, T. PZT Based Tunable Interdigital Transducer for Lamb Waves Based NDT and SHM. *Mech. Syst. Signal Process.* **2016**, *78*, 71–83, doi:10.1016/j.ymssp.2015.12.013.

83. Lugovtsova, Y.; Bulling, J.; Boller, C.; Prager, J. Analysis of Guided Wave Propagation in a Multi-Layered Structure in View of Structural Health Monitoring. *Appl. Sci.* **2019**, *9*, 4600, doi:10.3390/app9214600.

84. Giannelli, P.; Bulletti, A.; Capineri, L. Multifunctional Piezopolymer Film Transducer for Structural Health Monitoring Applications. *IEEE Sens. J.* **2017**, *17*, 4583–4586, doi:10.1109/JSEN.2017.2710425.

85. Marchi, L.D.; Testoni, N.; Marzani, A. Spiral-Shaped Piezoelectric Sensors for Lamb Waves Direction of Arrival (DoA) Estimation. *Smart Mater. Struct.* **2018**, *27*, 045016, doi:10.1088/1361-665X/aab19e.

86. Koduru, J.P.; Rose, J.L. Mode Controlled Guided Wave Tomography Using Annular Array Transducers for SHM of Water Loaded Plate like Structures. *Smart Mater. Struct.* **2013**, *22*, 125021, doi:10.1088/0964-1726/22/12/125021.

87. Gao, H. Ultrasonic Guided Wave Annular Array Transducers for Structural Health Monitoring. In Proceedings of the AIP Conference Proceedings; AIP: Brunswick, Maine (USA), 2006; Vol. 820, pp. 1680–1686.

88. Salowitz, N.P.; Kim, S.-J.; Kopsaftopoulos, F.; Li, Y.-H.; Chang, F.-K. Design and Analysis of Radially Polarized Screen-Printed Piezoelectric Transducers. *J. Intell. Mater. Syst. Struct.* **2017**, *28*, 934–946, doi:10.1177/1045389X16666177.

89. [No Title Found]. *J. Mech. Mater. Struct.* **15**.

90. Ren, B.; Lissenden, C. Phased Array Transducers for Ultrasonic Guided Wave Mode Control and Identification for Aircraft Structural Health Monitoring. *Mater. Eval.* **2015**, *73*, 1089–1100.

91. Aranguren, G.; Monje, P.M.; Cokonaj, V.; Barrera, E.; Ruiz, M. Ultrasonic Wave-Based Structural Health Monitoring Embedded Instrument. *Rev. Sci. Instrum.* **2013**, *84*, 125106, doi:10.1063/1.4834175.

92. Rathod, V.T. A Review of Electric Impedance Matching Techniques for Piezoelectric Sensors, Actuators and Transducers. *Electronics* **2019**, *8*, 169, doi:10.3390/electronics8020169.

93. Schubert, L.; Frankenstein, B.; Reppe, G. Match-X Based Microsystem for Structural Health Monitoring. In Proceedings of the 2006 1st Electronic Systemintegration Technology Conference; IEEE: Dresden, Germany, 2006; pp. 635–641.

94. Ferin, G.; Muralidharan, Y.; Mesbah, N.; Chatain, P.; Bantignies, C.; Hung Le Khanh; Flesch, E.; An Nguyen-Dinh Smart Autonomous Wireless Acoustic Sensors for Aeronautical SHM Applications. In Proceedings of the 2015 IEEE International Ultrasonics Symposium (IUS); IEEE: Taipei, Taiwan, October 2015; pp. 1–4.

95. Beattie, A. Acoustic Emission Non-Destructive Testing of Structures Using Source Location Techniques*.; 2013.

96. Ebrahimkhanlou, A.; Dubuc, B.; Salamone, S. A Generalizable Deep Learning Framework for Localizing and Characterizing Acoustic Emission Sources in Riveted Metallic Panels. *Mech. Syst. Signal Process.* **2019**, *130*, 248–272, doi:10.1016/j.ymssp.2019.04.050.

97. Yun, J. [Https://Vtechworks.Lib.vt.Edu/Handle/10919/42507](https://Vtechworks.Lib.vt.Edu/Handle/10919/42507) 2011.

98. Thomas, A.J.; Kim, J.J.; Tallman, T.N.; Bakis, C.E. Damage Detection in Self-Sensing Composite Tubes via Electrical Impedance Tomography. *Compos. Part B Eng.* **2019**, *177*, 107276, doi:10.1016/j.compositesb.2019.107276.

99. Boukabache, H.; Escriba, C.; Fourniols, J.-Y. Toward Smart Aerospace Structures: Design of a Piezoelectric Sensor and Its Analog Interface for Flaw Detection. *Sensors* **2014**, *14*, 20543–20561, doi:10.3390/s141120543.

100. Capineri, L.; Giannelli, P.; Calabrese, G. Comparison of Voltage-Mode and Charge-Mode Amplifiers for Interfacing Piezopolymer Transducers to SHM Electronic Systems. In Proceedings of the 2019 26th IEEE International Conference on Electronics, Circuits and Systems (ICECS); IEEE: Genoa, Italy, November 2019; pp. 278–281.

101. Ren, Y.; Qiu, L.; Yuan, S.; Su, Z. A Diagnostic Imaging Approach for Online Characterization of Multi-Impact in Aircraft Composite Structures Based on a Scanning Spatial-Wavenumber Filter of Guided Wave. *Mech. Syst. Signal Process.* **2017**, *90*, 44–63, doi:10.1016/j.ymssp.2016.12.005.

102. Capineri, L.; Bulletti, A.; Calzolai, M.; Francesconi, D. A Real-Time Electronic System for Automated Impact Detection on Aircraft Structures Using Piezoelectric Transducers. *Procedia Eng.* **2014**, *87*, 1243–1246, doi:10.1016/j.proeng.2014.11.408.

103. International Conference on Structural Health Monitoring and Integrity Management; Ding, K.; Yuan, S.; Wu, Z. *Structural Health Monitoring and Integrity Management*; CRC Press/Balkema: Leiden, The Netherlands, 2015; ISBN 978-1-315-69046-9.

104. Gao, F.; Zeng, L.; Lin, J.; Shao, Y. Damage Assessment in Composite Laminates via Broadband Lamb Wave. *Ultrasonics* **2018**, *86*, 49–58, doi:10.1016/j.ultras.2018.01.005.

105. Glaser, S.; Li, H.; Wang, M.; Ou, J.; Lynch, J. Sensor Technology Innovation for the Advancement of Structural Health Monitoring: A Strategic Program of US-China Research for the next Decade. *Smart Struct. Syst.* **2007**, *3*, 221–244, doi:10.12989/sss.2007.3.2.221.

106. Haller, M.I.; Khuri-Yakub, B.T. A Surface Micromachined Electrostatic Ultrasonic Air Transducer. *IEEE Trans. Ultrason. Ferroelectr. Freq. Control* **1996**, *43*, 1–6, doi:10.1109/58.484456.

107. Yaralioglu, G.G.; Degertekin, F.L.; Badi, M.H.; Auld, B.A.; Khuri-Yakub, B.T. Finite Element Method and Normal Mode Modeling of Capacitive Micromachined SAW and Lamb Wave Transducers. In Proceedings of the 2000 IEEE Ultrasonics Symposium. Proceedings. An International Symposium (Cat. No.00CH37121); IEEE: San Juan, Puerto Rico, 2000; Vol. 1, pp. 129–132.

108. Brenner, K.; Ergun, A.; Firouzi, K.; Rasmussen, M.; Stedman, Q.; Khuri-Yakub, B. Advances in Capacitive Micromachined Ultrasonic Transducers. *Micromachines* **2019**, *10*, 152, doi:10.3390/mi10020152.

109. Bradley, R.J. Capacitive Ultrasonic Transducers Fabricated Using Microstereolithography 2007.

110. BUTAUD, P.; Bourbon, G.; Le Moal, P.; Joseph, E.; Verdin, B.; Ramasso, E.; Placet, V. CMUT Sensors Based on Circular Membranes Array for SHM Applications. In Proceedings of the Smart Structures + Nondestructive Evaluation; Denver, United States, March 2019.

111. Savoia, A.S.; Caliano, G.; Pappalardo, M. A CMUT Probe for Medical Ultrasonography: From Microfabrication to System Integration. *IEEE Trans. Ultrason. Ferroelectr. Freq. Control* **2012**, *59*, 1127–1138, doi:10.1109/TUFFC.2012.2303.

112. Boubenia, R.; Bourbon, G.; Le Moal, P.; Joseph, E.; Ramasso, E.; Placet, V. Acoustic Emission Sensing Using MEMS for Structural Health Monitoring : Demonstration of a Newly Designed Capacitive Micro Machined Ultrasonic Transducer. In Proceedings of the 12th International Workshop on Structural Health Monitoring; Stanford, California, United States, September 2019.

113. Kabir, M.; Kazari, H.; Ozevin, D. Piezoelectric MEMS Acoustic Emission Sensors. *Sens. Actuators Phys.* **2018**, *279*, 53–64, doi:10.1016/j.sna.2018.05.044.

114. Ozevin, D. MEMS Acoustic Emission Sensors. *Appl. Sci.* **2020**, *10*, 8966, doi:10.3390/app10248966.

115. International Conference on Structural Health Monitoring of Intelligent Infrastructure *7th International Conference on Structural Health Monitoring of Intelligent Infrastructure (SHMII 2015)*; Torino, Italy, July 1-3, 2015; De Stefano, A., Ed.; Curran Associates, Inc: Red Hook, NY, 2016; ISBN 978-1-5108-2107-1.

116. Güemes, A.; Fernandez-Lopez, A.; Pozo, A.R.; Sierra-Pérez, J. Structural Health Monitoring for Advanced Composite Structures: A Review. *J. Compos. Sci.* **2020**, *4*, 13, doi:10.3390/jcs4010013.

117. Perçin, G.; Atalar, A.; Levent Degertekin, F.; Khuri-Yakub, B.T. Micromachined Two-Dimensional Array Piezoelectrically Actuated Transducers. *Appl. Phys. Lett.* **1998**, *72*, 1397–1399, doi:10.1063/1.121067.

118. Muralt, P.; Kholkin, A.; Kohli, M.; Maeder, T. Piezoelectric Actuation of PZT Thin-Film Diaphragms at Static and Resonant Conditions. *Sens. Actuators Phys.* **1996**, *53*, 398–404, doi:10.1016/0924-4247(96)01139-9.

119. Bernstein, J.J.; Finberg, S.L.; Houston, K.; Niles, L.C.; Chen, H.D.; Cross, L.E.; Li, K.K.; Udayakumar, K. Micromachined High Frequency Ferroelectric Sonar Transducers. *IEEE Trans. Ultrason. Ferroelectr. Freq. Control* **1997**, *44*, 960–969, doi:10.1109/58.655620.

120. Feng, G.-H.; Chen, W.-M. Micromachined Lead Zirconium Titanate Thin-Film-Cantilever-Based Acoustic Emission Sensor with Poly(N-Isopropylacrylamide) Actuator for Increasing Contact Pressure. *Smart Mater. Struct.* **2016**, *25*, 055046, doi:10.1088/0964-1726/25/5/055046.

121. Farrar, C.R.; Park, G.; Todd, M.D. Sensing Network Paradigms for Structural Health Monitoring. In *New Developments in Sensing Technology for Structural Health Monitoring*; Mukhopadhyay, S.C., Ed.; Lecture Notes in Electrical Engineering; Springer Berlin Heidelberg: Berlin, Heidelberg, 2011; Vol. 96, pp. 137–157 ISBN 978-3-642-21098-3.

122. IEEE Aerospace Conference; IEEE Aerospace and Electronic Systems Society; American Institute of Aeronautics and Astronautics 2007 *IEEE Aerospace Conference Digest: Big Sky, Montana, March 3-10, 2007*; IEEE: Piscataway, N.J., 2007;

123. Fu, H.; Sharif Khodaei, Z.; Aliabadi, M.H.F. An Event-Triggered Energy-Efficient Wireless Structural Health Monitoring System for Impact Detection in Composite Airframes. *IEEE Internet Things J.* **2019**, *6*, 1183–1192, doi:10.1109/JIOT.2018.2867722.

124. Overly, T.G.S.; Park, G.; Farinholt, K.M.; Farrar, C.R. Development of an Extremely Compact Impedance-Based Wireless Sensing Device. *Smart Mater. Struct.* **2008**, *17*, 065011, doi:10.1088/0964-1726/17/6/065011.

125. Giannì, C.; Balsi, M.; Esposito, S.; Ciampa, F. Low-power Global Navigation Satellite System-enabled Wireless Sensor Network for Acoustic Emission Localisation in Aerospace Components. *Struct. Control Health Monit.* **2020**, *27*, doi:10.1002/stc.2525.

126. Mateu, L.; Moll, F. Review of Energy Harvesting Techniques and Applications for Microelectronics (Keynote Address); Lopez, J.F., Fernandez, F.V., Lopez-Villegas, J.M., de la Rosa, J.M., Eds.; Sevilla, Spain, June 30 2005; pp. 359–373.

127. Sodano, H.A.; Inman, D.J.; Park, G. A Review of Power Harvesting from Vibration Using Piezoelectric Materials. *Shock Vib. Dig.* **2004**, *36*, 197–205, doi:10.1177/0583102404043275.

128. Ferrari, M.; Ferrari, V.; Guizzetti, M.; Andò, B.; Baglio, S.; Trigona, C. Improved Energy Harvesting from Wideband Vibrations by Nonlinear Piezoelectric Converters. *Sens. Actuators Phys.* **2010**, *162*, 425–431, doi:10.1016/j.sna.2010.05.022.

129. Park, G.; Farinholt, K.M.; Farrar, C.R.; Rosing, T.; Todd, M.D. Powering Wireless SHM Sensor Nodes through Energy Harvesting. In *Energy Harvesting Technologies*; Priya, S., Inman, D.J., Eds.; Springer US: Boston, MA, 2009; pp. 493–506 ISBN 978-0-387-76463-4.

130. Zelenika, S.; Hadas, Z.; Bader, S.; Becker, T.; Gluščić, P.; Hlinka, J.; Janak, L.; Kamenar, E.; Ksica, F.; Kyratsi, T.; et al. Energy Harvesting Technologies for Structural Health Monitoring of Airplane Components—A Review. *Sensors* **2020**, *20*, 6685, doi:10.3390/s20226685.

131. Ferrari, M.; Ferrari, V.; Guizzetti, M.; Marioli, D. An Autonomous Battery-Less Sensor Module Powered by Piezoelectric Energy Harvesting with RF Transmission of Multiple Measurement Signals. *Smart Mater. Struct.* **2009**, *18*, 085023, doi:10.1088/0964-1726/18/8/085023.

132. [Www.Metisdesign.Com](http://www.metisdesign.com).

133. [Http://cordis.europa.eu/project/rcn/108855_en.html](http://cordis.europa.eu/project/rcn/108855_en.html).

134. Smithard, J.; Norman, P.; van der Velden, S.; Powlesland, I.; Jung, G.; Rajic, N.; Galea, S. The Acousto Ultrasonic Structural Health Monitoring Array Module (AUSAM +) for Damage Detection in Structures. *Procedia Eng.* **2017**, *188*, 448–455, doi:10.1016/j.proeng.2017.04.507.

135. JU, Z.; Li, F.; JANAPATI, V.; Chung, H.; Yadav, S.; CHEUNG, C. *Sensor Network Design Technique for Monitoring Railroad Structures*; 2016;

136. Sundaram, B.A.; Ravisankar, K.; Senthil, R.; Parivallal, S. Wireless Sensors for Structural Health Monitoring and Damage Detection Techniques. *Curr. Sci.* **2013**, *104*, 1496–1505.

137. Ren, Y.; Yuan, S.; Qiu, L.; Mei, H. Impact Localization by a Multi-Radio Sink-Based Wireless Sensor Network for Large-Scale Structures. *Adv. Struct. Eng.* **2017**, *20*, 157–169, doi:10.1177/1369433216660005.

138. Testoni, N.; Aguzzi, C.; Arditi, V.; Zonzini, F.; De Marchi, L.; Marzani, A.; Cinotti, T.S. A Sensor Network with Embedded Data Processing and Data-to-Cloud Capabilities for Vibration-Based Real-Time SHM. *J. Sens.* **2018**, *2018*, 1–12, doi:10.1155/2018/2107679.

139. Mascareñas, D.; Cattaneo, A.; Theiler, J.; Farrar, C. Compressed Sensing Techniques for Detecting Damage in Structures. *Struct. Health Monit. Int. J.* **2013**, *12*, 325–338, doi:10.1177/1475921713486164.

140. Arcadius Tokognon, C.; Gao, B.; Tian, G.Y.; Yan, Y. Structural Health Monitoring Framework Based on Internet of Things: A Survey. *IEEE Internet Things J.* **2017**, *4*, 619–635, doi:10.1109/JIOT.2017.2664072.

141. Scuro, C.; Sciammarella, P.F.; Lamonaca, F.; Olivito, R.S.; Carni, D.L. IoT for Structural Health Monitoring. *IEEE Instrum. Meas. Mag.* **2018**, *21*, 4–14, doi:10.1109/MIM.2018.8573586.

142. Muttillo, M.; Stornelli, V.; Alaggio, R.; Paolucci, R.; Di Battista, L.; de Rubeis, T.; Ferri, G. Structural Health Monitoring: An IoT Sensor System for Structural Damage Indicator Evaluation. *Sensors* **2020**, *20*, 4908, doi:10.3390/s20174908.

143. Abdelgawad, A.; Yelamarthi, K. Internet of Things (IoT) Platform for Structure Health Monitoring. *Wirel. Commun. Mob. Comput.* **2017**, *2017*, 1–10, doi:10.1155/2017/6560797.

144. IEEE Staff *2018 IEEE 4th World Forum on Internet of Things (WF IoT)*; IEEE: Piscataway, 2018; ISBN 978-1-4673-9945-6.

145. Worden, K.; Baldacchino, T.; Rowson, J.; Cross, E.J. Some Recent Developments in SHM Based on Nonstationary Time Series Analysis. *Proc. IEEE* **2016**, *104*, 1589–1603, doi:10.1109/JPROC.2016.2573596.

146. Bao, Y.; Chen, Z.; Wei, S.; Xu, Y.; Tang, Z.; Li, H. The State of the Art of Data Science and Engineering in Structural Health Monitoring. *Engineering* **2019**, *5*, 234–242, doi:10.1016/j.eng.2018.11.027.

147. Yuan, F.-G.; Zargar, S.A.; Chen, Q.; Wang, S. Machine Learning for Structural Health Monitoring: Challenges and Opportunities. In Proceedings of the Sensors and Smart Structures Technologies for Civil, Mechanical, and Aerospace Systems 2020; Zonta, D., Sohn, H., Huang, H., Eds.; SPIE: Online Only, United States, April 23 2020; p. 2.

148. Hesser, D.F.; Kocur, G.K.; Markert, B. Active Source Localization in Wave Guides Based on Machine Learning. *Ultrasonics* **2020**, *106*, 106144, doi:10.1016/j.ultras.2020.106144.

149. Mariani, S.; Rendu, Q.; Urbani, M.; Sbarufatti, C. Causal Dilated Convolutional Neural Networks for Automatic Inspection of Ultrasonic Signals in Non-Destructive Evaluation and Structural Health Monitoring. *Mech. Syst. Signal Process.* **2021**, *157*, 107748, doi:10.1016/j.ymssp.2021.107748.

150. Sun, L.; Shang, Z.; Xia, Y.; Bhowmick, S.; Nagarajaiah, S. Review of Bridge Structural Health Monitoring Aided by Big Data and Artificial Intelligence: From Condition Assessment to Damage Detection. *J. Struct. Eng.* **2020**, *146*, 04020073, doi:10.1061/(ASCE)ST.1943-541X.0002535.
151. Melville, J.; Alguri, K.S.; Deemer, C.; Harley, J.B. Structural Damage Detection Using Deep Learning of Ultrasonic Guided Waves.; Provo, Utah, USA, 2018; p. 230004.

Appendix A

Acronym

AAF	Anti Aliasing Filter
ADC	Analog to Digital Converter
AFE	Analog Front-End
AI	Artificial Intelligence
AIC	Akaike Information Criterion
AlN	Aluminum Nitride
ANN	Artificial Neural Network
ASCS	Aircraft Smart Composite Skin
ASIC	Application Specific Integrated Circuit
BD	Big Data
BSS	Bioinspired Stretchable Sensors
CAN	Controller Area Network
CFRP	Composite Fiber Reinforce Polymer
CMRR	Common Mode Rejection Ratio
CMUT	Capacitive Micromachined Ultrasonic Transducer
CNN	Convolutanional Neural Network
CNT	Carbon Nanotubes
COPV	Composite Overwrapped Pressure Vessel
COTS	Component Of The Shelf
CWT	Continuous Wavelet Transform
DSP	Digital Signal Processor
DToA	Differential Time of Arrival
EMI	Electro-Mechanical Impedance
FBG	Fiber Bragg Grating
FPC	Flexible printed circuit
FPGA	Field Programmable Gate Array
FUT	Flexible Ultrasonic Transducers
GFRP	Glass Fiber Reinforced Polymer
IDT	Interdigital Transducer
INA	Instrumentation Amplifier
IoT	Internet of Things
ISHM	Integrated Structural Health Monitoring
LNA	Low Noise Amplifier
MEMS	Micro Electrical Mechanical System
MFC	Macro Fiber Composite
ML	Machine Learning
NDI	Non Destructive Inspection
NDT	Non Destructive Testing
NF	Noise Figure
PLC	Power Line Communication

PMUT	Piezoelectric Micromachined Ultrasonic Transducers
PTP	Precise Time Protocol
PVDF	Polyvinylidene fluoride
PVDF-TrFE	Polyvinylidene difluoride–trifluoroethylene copolymer
PZT	Lead zirconate titanate
PWAS	Piezoelectric Wafer Active Sensors
ROI	Region Of Interest
RPL	Routing protocols for low-power networks
RTD	Resistive Temperature Device
SH	Shear Horizontal
SHM	Structural Health Monitoring
SiC	Silicon Carbide
SL	SMART Layer®
SS	Smart-Skin
SLDV	Scanning Laser Doppler Vibrometer
SNR	Signal to Noise Ratio
SOC	System on Chip
STFT	Short Time Fourier Transform
TOF	Time Of Flight
UGM	Ultrasonic Guided Mode
UGW	Ultrasonic Guided Wave
VGA	Variable Gain Amplifier
WSN	Wireless Sensor Network

Author's contributions

L. Capineri has defined the motivations and layout of this review paper, focussing on the most innovative topics. A. Bulletti has collected the pictures and data to complete the sections and organized the references.